ALLIS-CHALMERS

Electrical REVIEW

1ST QUARTER 1954

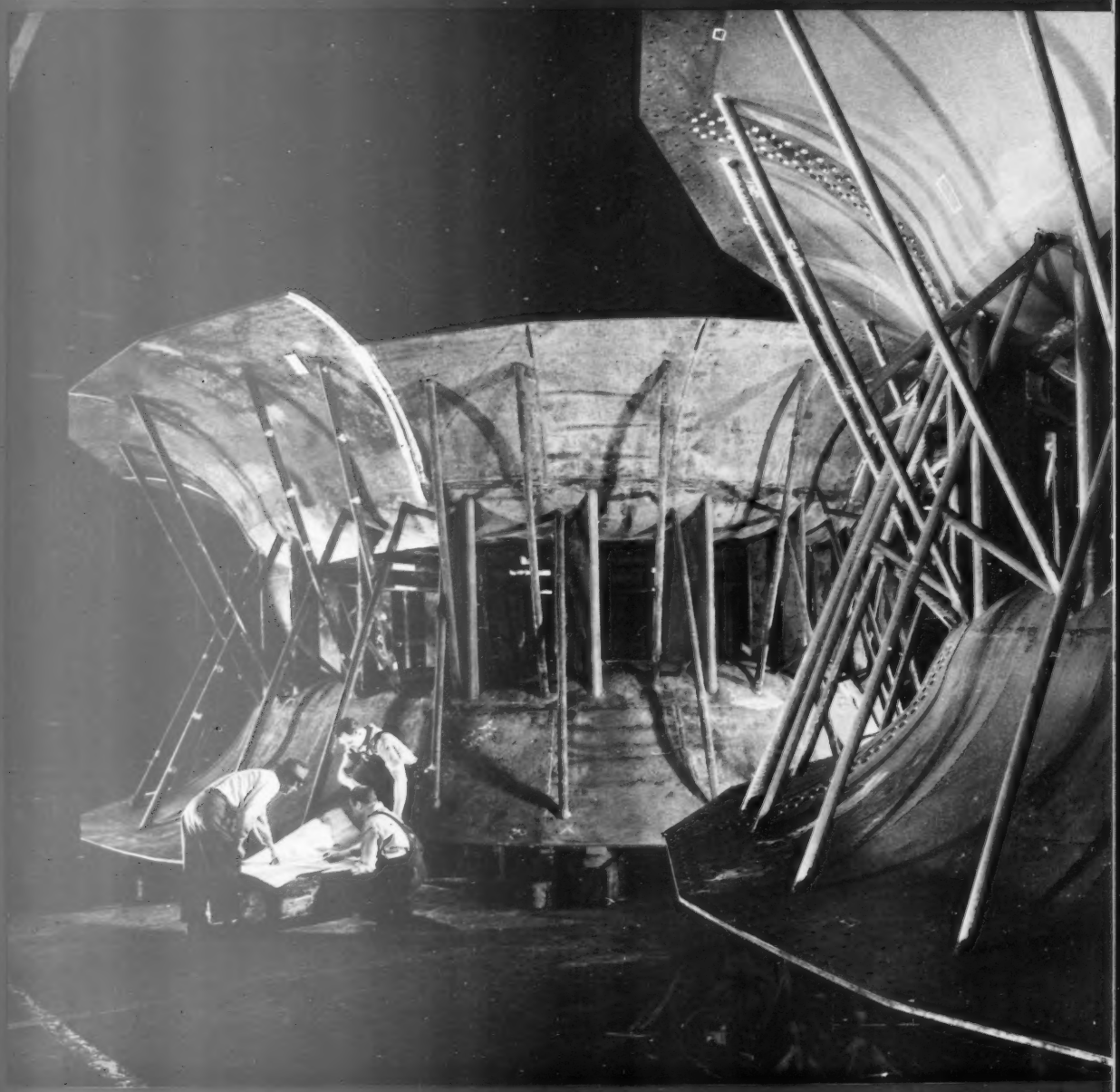

5/8% STEP VOLTAGE REGULATORS

AFTER 17 YEARS' OPERATION

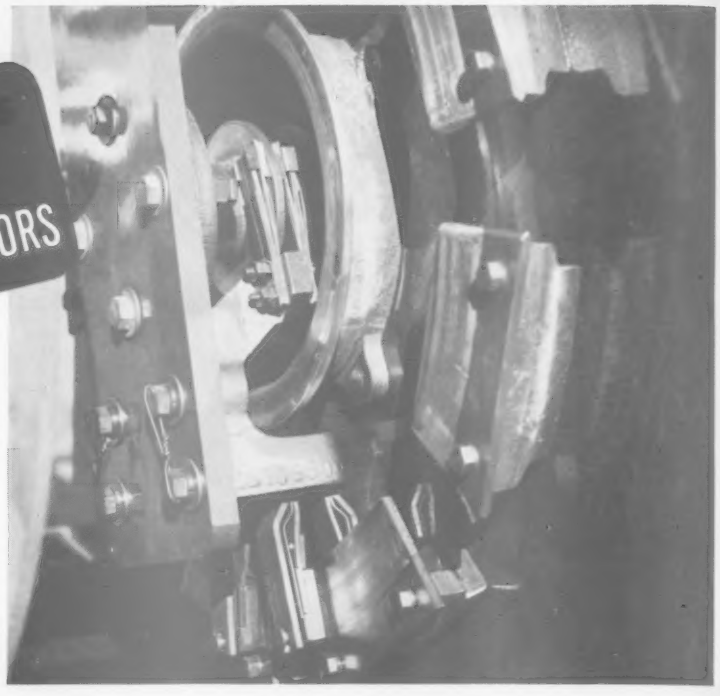

Practically No Wear!

The unretouched photo above shows the condition of the tap changer from an Allis-Chalmers power regulator that has changed taps 1,240,000 times on a western utility.

You can see from this photo that this regulator is still in excellent condition — it will give many more years of satisfactory service.

This 17-year operating record adds field proof to laboratory tests that have shown that the *Quick-Break* mechanism will withstand five million operations. You get this rugged, reliable mechanism on every Allis-Chalmers ⅝% step voltage regulator. It gives fast, clean wiping action that snaps moving contacts from one stationary contact to the next before there is time for damage to occur.

In addition, when you depend on Allis-Chalmers, you benefit from more than twenty years' experience building ⅝% step voltage regulators. No other manufacturer gives you this kind of design and operating experience.

Next time you consider regulation, for new or replacement installations, it will pay to get the complete facts about Allis-Chalmers regulators. Contact your nearby A-C district office or write Allis-Chalmers, Milwaukee 1, Wisconsin, for more details.

A-4242

Single-Phase Power Regulator

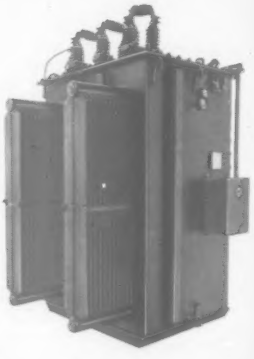

Three-Phase Power Regulator

Single-Phase Distribution Regulator

ALLIS-CHALMERS

Originators of ⅝% Step Regulation

A-C ALLIS-CHALMERS

ALLIS-CHALMERS Electrical REVIEW

THE COVER

SUBTERRANEAN CAROUSEL—Circling water racing through spiral casings will be directed by these stay-ring assemblies into Francis type runners where 57,500 hp will be harnessed by each of eight identical hydraulic turbines drawing water through 22-ft diameter inlets under 112-ft head from the 6,300,000 acre-feet Fort Randall Reservoir in southeastern South Dakota. Since the dedication on March 15th, one turbine in this U.S. Army Corps of Engineers' multipurpose dam project has been in operation — seven others are in various stages of installation, construction, and manufacture.

A-C Staff Photo by M. Durante

Allis-Chalmers

ELECTRICAL REVIEW

Vol. XIX No. 1

Executive Board

R. M. Casper F. W. Bush
A. R. Tofte

Editor...G. C. Quinn

Assistant Editor.....R. W. Smeaton
Managing Editor.....R. S. Bloor
Technical Editor.....W. L. Peterson

Associate Editors: P. Castner, J. A. Zimmerman, O. Keller, M. C. Maloney, T. B. Montgomery, J. E. Kerwin, B. A. Storaasli, F. Smeltz, J. A. Keymar, E. A. Kilgour, W. D. Dineen.

Layout Artist: L. Schallock.
Circulation: John Gumtz.

Issued quarterly. Subscription rates: U. S., Mexico, and Canada, $2.00 per year; other countries, $3.00; single copies, $1.00 in advance.

CONTENTS

Progress Report...Supercharged Cooling Today.... 4
L. T. ROSENBERG

Seal and Bearing Testing of Modern Generators.... 8
FRED A. BERMKE

Regulators vs. Switched Capacitors..... 10
R. D. OKERBERG

Auxiliary Drive Motor Keeps Pace with Modern Power 16
C. D. LAWTON

Ion Exchange — Electrochemistry's New Frontier.... 22
T. L. PANKEY

Corona-Free Switchgear 26
CARL MERCIER

A Design Philosophy for General Purpose Motors... 35
V. B. HONSINGER

Indexed regularly by Engineering Index, Inc.
Allis-Chalmers ELECTRICAL REVIEW is available to public and institutional libraries on microfilm from University Microfilms, 313 N. First St., Ann Arbor, Mich.

Address Allis-Chalmers Electrical Review, Milwaukee 1, Wisconsin

Printed in U. S. A.

Copyright 1954 by Allis-Chalmers Mfg. Co.

PROGRESS REPORT . . .

Supercharged Cooling Today!

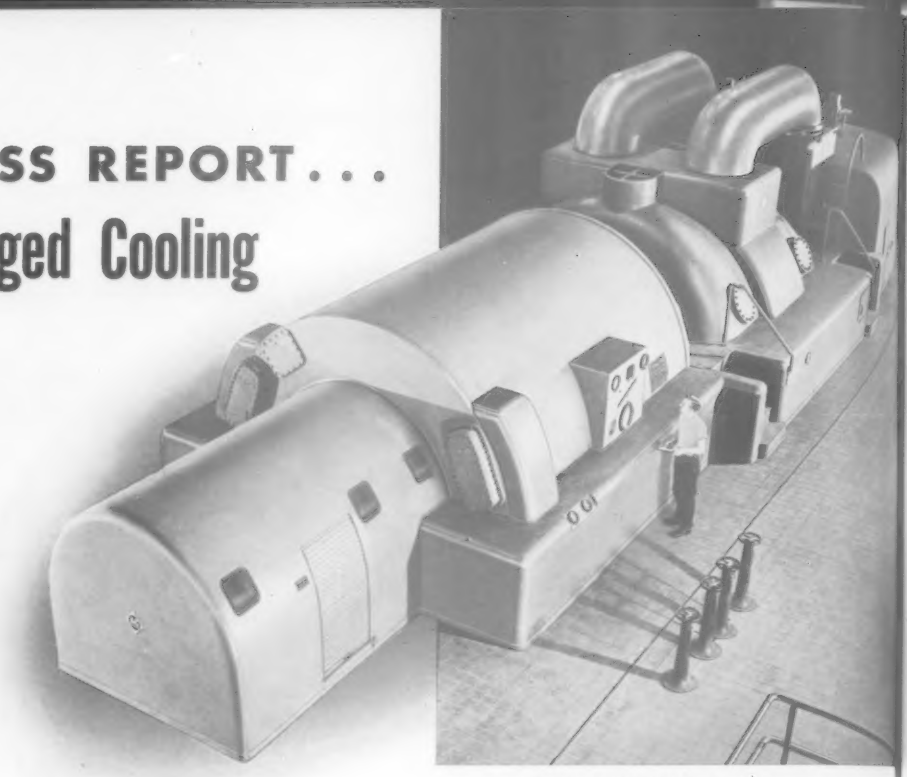

SPACE REQUIREMENTS, crane capacity, and other power-plant costs were materially reduced by supercharging the rotor of this 88,235-kva at 30 psig machine. **(FIG. 1)**

by L. T. ROSENBERG
Motor and Generator Section
Allis-Chalmers Mfg. Co.

Nearly three years of on-the-line experience proves the barrier to effective generator cooling has been overcome.

THE INTRODUCTION of supercharged internal conductor cooling of steam turbine generators in July, 1951, was a great forward step in the long chain of ventilation developments extending over the past half century. As high speed turbine units grew in size the generator rotor had to be made longer because mechanical strength considerations limited the diameter. As a result, both the stator and rotor became increasingly difficult to ventilate.

Stator cooling advanced ahead of rotor cooling, first in 1924 by virtue of multiple radial air flow,[1] utilizing the space surrounding the core, and in 1937, by means of spiral ventilation,[2] in which successive radial passages along the core length became alternately inlets and outlets. Rotor advances depended mainly on improved physical and magnetic properties of forgings, and such details as grooved outer surfaces, trenches below the rotor coils, radial air gap scoops,[1] and axial ducts along the teeth and poles. The adoption of hydrogen cooling at ½ psig added another 20 to 25 percent to machine capacity. Raising hydrogen pressure to 30 psig yielded approximately an additional 19 percent capacity when corrected for normal short circuit ratio.

In contrast to these modest improvements, the application of supercharging to the rotor alone in 1951 added 65 percent to the output per pound of rotor weight at ½ psig hydrogen and with normal short circuit ratio. Complete supercharging of the stator as well as the rotor, when coupled with the greater benefits obtainable from gas pressures of 30 psig and higher, adds another large step to the output per pound of material.

Application of the cooling medium directly to the copper conductors is not without precedent. The bare strap copper field coils of salient pole machines have been successfully cooled for years, with beveled edges providing increased surface area exposed to the air. The end portions of turbine generator rotor coils have likewise been left partly exposed to the cooling medium with good results.

Early attempts to carry the coolant into the slot portion proved impractical or did not provide sufficiently important gains, probably due to the lack of one or more of the following essential components of supercharged cooling:

(a) A blower capable of developing several times the normal fan pressure used with conventional cooling.

(b) A cooling gas (such as hydrogen) sealed against contamination and capable of being circulated with moderate blower power and temperature rise due to blower losses.

(c) Duct design (in conjunction with the blower) that insures more than the minimum threshold mass flow of coolant to prevent excessive gas temperature rise.

(d) Ample copper surface exposed to the coolant to transfer the heat generated with a small temperature drop.

(e) High gas velocity over the copper surface to improve the surface heat transfer coefficient.

(f) Adequate mechanical support along the sides of the conductors to prevent distortion from thermal expansion forces.

Figure 1 shows a recently installed, 60,000-kw turbine-generator unit having a supercharged rotor. In this type of machine, a two-stage blower forces hydrogen at high velocity through ducts in the rotor copper, whose surface area has been increased by the beveled conductor design shown in Figure 2. The successive rotor turns combine in pairs to share a common pair of ducts having a larger hydraulic radius and consequently lower duct friction than would be possible within a single turn. This design, although costly to manufacture, affords easy entry of gas into the ducts, low resistance to gas flow, and facility for duct inspection without removal of rotor coils. The conductor is continuously supported mechanically throughout its length, and its overhung beveled edges are designed for maximum overspeed stresses.

With cool hydrogen entering the rotor copper at both ends, a more effective cooling means had to be found for the slot region in order to avoid excessive temperature at the center of the rotor. This was accomplished by admitting most of the compressed hydrogen into the conductors where the conductors enter the slots. Only a minor portion is allowed to flow in the coil ends. As a result, the rotor temperature rise distribution is as shown in Figure 3. The spread between hot spot and average temperature is not appreciably different from that of a conventionally cooled machine of the same rating but correspondingly longer length. Calculations and tests indicate a rise of 85 C by resistance to be safe for supercharged rotors of this type.

Rotor supercharging proves itself

The first partially supercharged machine has already completed 2½ years of operation. During the calendar years 1952 and 1953, this generating unit had an availability record of 99.86 percent. The brief outages were due to minor factors not involving the generator. Although nominally rated at ½ psig hydrogen pressure, a 60,000-kw unit of this type saves about 9 feet of power plant space compared to a conventional machine of the same rating. Its reduced length and lighter weight result in numerous advantages in reduced thermal expansion, foundation and crane costs, and other savings. Although its maximum load with higher gas pressure is limited by the conventionally cooled stator coils to 125 percent at 30 psig, the rotor becomes extremely cool as pressure is raised.

This outstanding behavior of the supercharged machine at elevated pressure results mainly from the virtual elimination of the heat flow through the insulation wall. The temperature gradient through the insulation of a conventional machine accounts for the major component of the copper temperature rise, yet it is substantially independent of the hydrogen pressure and hence will increase with overloads despite pressure increase. The minor components — gas rise and contact surface rise — that do respond to gas pressure are insignificant at 30 psig. Hence, no great improvement can be achieved above 30 pounds with conventional cooling.

With supercharged cooling, practically no heat flows through the insulation; and the major component of copper temperature rise is the gas rise, which varies inversely with absolute pressure. Moreover, the coefficient of heat transfer between copper and hydrogen also improves with pressure. Hence, this characteristic of continued improvement with increasing hydrogen pressures up to 100 psig or higher is an inherent feature of this new cooling method.

As stated in previous papers,[3, 4] to take full advantage of this new principle, the thermal barrier of the stator coil insulation would also have to be removed. Consequently, the construction of the fully supercharged generator shown in Figure 4 was undertaken.

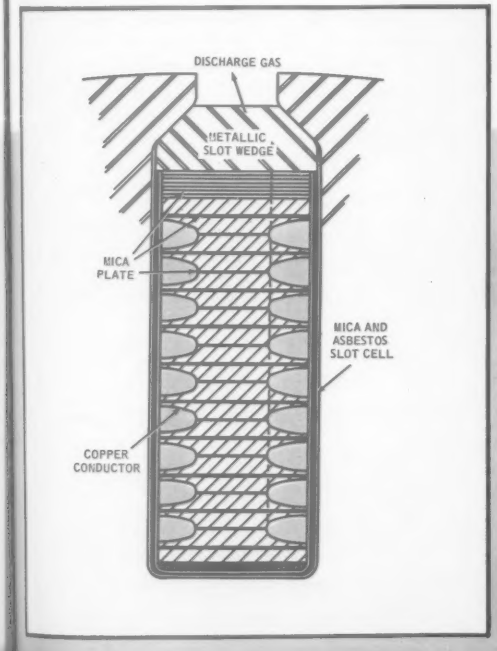

LARGE CONTACT AREA for the fast-moving hydrogen in the ducts, shown in color, result from the unique rotor conductor shape. **(FIGURE 2)**

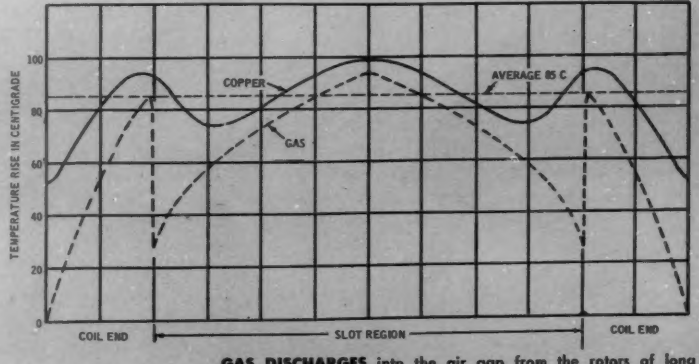

GAS DISCHARGES into the air gap from the rotors of long machines, resulting in this temperature distribution. A maximum-to-average temperature ratio below 1.2 is achieved. **(FIGURE 3)**

COMPACT ARRANGEMENT of the fully supercharged machine not only saves hydrogen and CO_2 when scavenging, but also permits shipment of the largest ratings fully assembled. **(FIGURE 4)**

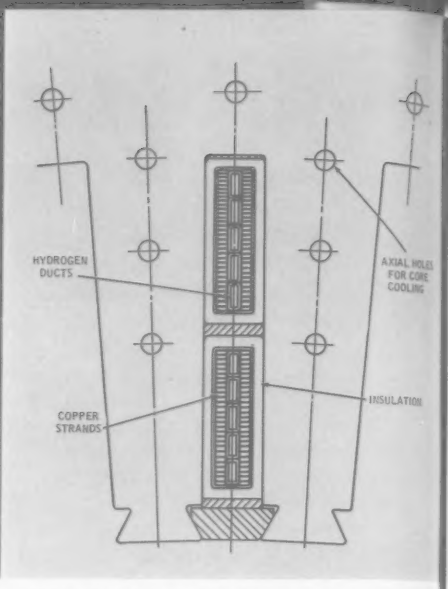

STATOR-COOLING PASSAGES are proportioned to minimize duct friction and assure intimate contact with every conductor strand. **(FIGURE 5)**

Stator supercharging simplifies ventilation

This first completely supercharged unit is rated 40 mw at 30 psig hydrogen pressure, with still greater capability ratings at higher pressures. Since both the stator and rotor are cooled from one end to the other, the ventilation circuit is simpler than for the partially supercharged design. A single-stage blower has been developed capable of the same fan pressure as the earlier two-stage design. The hydrogen discharged from the blower enters the coolers at the outboard end and, after being cooled, re-enters the generator at the turbine end. From this point, the flow is in straight parallel paths through rotor windings, air gap, stator coils, and core. With this design neither the blower loss nor the heat of compression is absorbed by the gas until after it has left the windings.

Stator coil cooling is illustrated in Figure 5. Rectangular metal tubes carry the high velocity hydrogen into close proximity to the stator copper strands. Tube and strand insulation are selected for low thermal resistance. The entire coil, including its ducts, is taped with full Class B insulation as is used on conventional coils. Since the tubes are at coil potential, special provision is made for adequate flashover and creepage distances where they emerge at the coil ends.

The stator core is cooled through numerous axial holes punched into the laminations. The number and size of these holes are so proportioned, relative to the ducts in the coils, that the stator core temperature will be nearly equal to that of the copper at full load. Differential thermal expansion between copper and iron is restricted by this means, and the major supply of hydrogen is conserved for the coils. This type of core cooling, together with a new external cooler arrangement, made it possible to greatly reduce the outer shell diameter of machines using this design and thus achieve a gas volume reduction of 5:1. The small diameter also permits shipment of larger machine ratings completely assembled.

Straight-through ventilation no hardship

Contrary to common expectations, the flow of coolant from one end of the generator to the other introduces no new problems either in hot-spot temperature or mechanical stress due to thermal expansion. The detectors in the fully supercharged generator are at the discharge end and will register very nearly equal to the hot-spot copper temperature even at pressures of 45 psig or higher. A 60 C rise by detector on such a machine would be safer than on a conventional machine with its usual temperature gradient through the insulation wall. Moreover, since each stator coil is much cooler at the turbine end, average temperature will likewise be lower than for a conventional coil, and thermal expansion less as a result.

For this type of end-to-end rotor coil ventilation, the maximum temperatures at the discharge end are appreciably lowered by staggering of inlets and outlets on the two sides of the same conductors and making use of the principle of partial gas entry into the coil ends. This increases copper temperature somewhat at the cool end, but the ratio of maximum to average can be held as low as 1.28 with this design, as shown in the lower curves of Figure 6.

Inequality in temperatures between the ends of a machine is in no way harmful so long as the temperature difference between copper and iron at each end is substantially the same, and the hot end temperature is known to be safe. Temperature distribution tests on full size model coils of the type used in the fully supercharged generator indicate that 30 psig will probably not be required for rated load.

Supercharging improves reactances and steady-state stability

The reactances of 3600-rpm partially and completely supercharged machines are compared with those of a conventional unit in Table I. It will be noted that the fully super-

TABLE I

	Conventional	Rotor Supercharged	Fully Supercharged
Power Factor	.85	.85	.85
Short Circuit Ratio	.8	.8	.8
x_d	1.44	1.47	1.55
x'_d	.15	.20	.25
x''_d	.08	.12	.135
x_2	.08	.12	.135
x_o	.02	.03	.035

REACTANCES with short circuit ratio based on usual ½ psig rating.

charged generator has reactances about the same as for a conventional 1800-rpm unit. These high reactances will permit less costly switchgear and reduce injury likely to occur at the point of a fault or from mechanical forces.

To maintain the customary high short circuit ratio, the air gap of the supercharged machine is increased and its operating flux density is raised about 10 percent above normal. This latter measure increases saturation and results in an important improvement in steady-state stability. The excitation requirements, however, are more than doubled.

It was partly because of this and partly because of a long felt need for greater exciter and regulator reliability that a separate research project was undertaken in an effort to raise the dependability level of the excitation system. The new, commutatorless excitation system, soon to be announced, serves also as a voltage regulator of superior speed of action and reliability.

Future outlook promising

Although best suited to 3600-rpm units because of the favorable blower speed, supercharging may ultimately be adapted for 1800-rpm generators as well, possibly with separately driven blowers. There is little doubt that most large 3600-rpm generators of the future will be cooled by forcing the cooling medium through ducts within the insulation wall because of the advantages to the user. Complete supercharging takes full advantage of elevated gas pressure and avoids the hazards of differential expansion by virtue of (a) shorter length, (b) lower temperature drop through insulation, and (c) lower average temperature. The compact design of the supercharged generator conserves hydrogen and facilitates shipment, while its reduced weight and length decrease bearing and seal maintenance, and building, crane, and foundation costs.

The higher saturation made possible by the new cooling principle improves steady-state stability, and the problem of increased excitation has been solved by a new commutatorless exciter-regulator. The higher reactances of supercharged machines afford a welcome return of the moderate fault currents and low circuit breaker interrupting requirements of the days of four-pole turbine generators.

BIBLIOGRAPHY

1. "A 115,000-Kw Turbo Alternator," R. B. Williamson, AIEE *Transactions,* September, 1932, p. 652.
2. "New Trends in Turbo-Generators," L. T. Rosenberg, Allis-Chalmers *Electrical Review,* Fourth Quarter, 1950.
3. "Supercharged Cooling of Generators," Sterling Beckwith, Allis-Chalmers *Electrical Review,* Third Quarter, 1951, p. 4.
4. "Supercharged Hydrogen Cooling of Generators," Sterling Beckwith, AIEE *Transactions,* Vol. 71, 1952.
5. "A New Fully Supercharged Generator," Sterling Beckwith and L. T. Rosenberg, AIEE Winter Meeting, New York, Jan. 19, 1954, Paper No. 54-48.
6. "Additional Design Features of the Fully Supercharged Generator," G. W. Staats and B. M. Koetting, AIEE Winter Meeting, New York, Jan. 19, 1954, Paper No. 54-92.

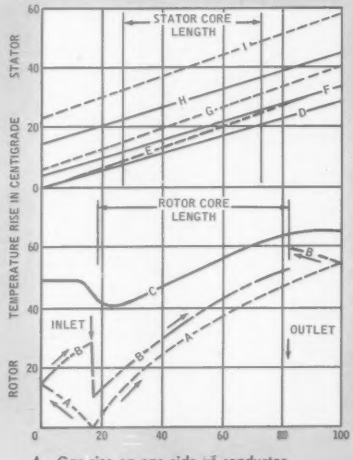
STATOR CORE LENGTH
ROTOR CORE LENGTH
STATOR
ROTOR
TEMPERATURE RISE IN CENTIGRADE
INLET
OUTLET
A Gas rise on one side of conductor.
B Gas rise on other side of conductor.
C Rotor copper temperature rise.
D Stator gas rise at 30 psig, full load.
E Stator gas rise at 45 psig, 1¼ load.
F Stator duct rise at 30 psig, full load.
G Stator duct rise at 45 psig, 1¼ load.
H Stator copper rise at 30 psig, full load.
I Stator copper rise at 45 psig, 1¼ load.

TEMPERATURE DISTRIBUTION along the length of the fully supercharged machine indicates maximum temperatures well within accepted limits. **(FIGURE 6)**

SHORTER LENGTH reduces thermal expansion of rotor and stator windings 40 percent, while internal cooling reduces rotor copper expansion forces another 25 percent in this 93,000-kva at 30 psig supercharged rotor machine. **(FIG. 7)**

Seal and Bearing Testing of MODERN GENERATORS

by **FRED A. BERMKE**
Plant Engineering
Allis-Chalmers Mfg. Co.

CONTINUOUSLY FILTERED OIL protects bearings and seals of large machines being tested in this new test facility. A 30,000-kva, 3000-rpm rotor is shown being balanced. The portable control console governs the oil pressure and flow to the bearings and seals. The control cabinet in the background contains all of the necessary auxiliary devices to assure proper operation of the test equipment.

SUPERCHARGED COOLING and other design changes have so improved the thermal capacity of hydrogen-cooled turbine generators that ratings of future units will soon be more than twice that of equivalent size present-day machines. Along with supercharged cooling, higher hydrogen pressures have contributed greatly to this revolutionary increase in thermal capacity.

To keep ahead of generator design changes, it has been necessary to anticipate operating conditions far enough in advance to provide adequate test facilities. A look at a new generator test pit will indicate clearly the designers' aims for the near future.

In the past decade, hydrogen pressures in standard machines increased from 3 to 30 psi. Now, designers are looking to pressures of 100 psi and over. When it became obvious that new designs would require these higher pressures, plans were immediately made to provide a new test pit that could supply sufficient oil at a high enough pressure to maintain the hydrogen seals. The resulting facility incorporated a number of interesting features which show the complexity of just one test pit in a large, modern, rotating machinery test floor.

Because the seal oil pressure supplied to the machine under test must be slightly higher than the operating hydrogen pressure, the equipment provides oil at pressures exceeding 100 psi, together with the automatic devices needed in a versatile, well-protected test layout. Up to 130 gpm of continuously filtered oil can be supplied to the seals under test at this pressure.

The bearing oil supply, too, has been designed to take care of future needs. Over 200 gpm of cooled and filtered oil at 20 psi is available for bearing oil supply.

Shown in the illustrations is some of the elaborate equipment used to provide an unfailing oil supply for the bearings and seals during normal generator tests and balancing.

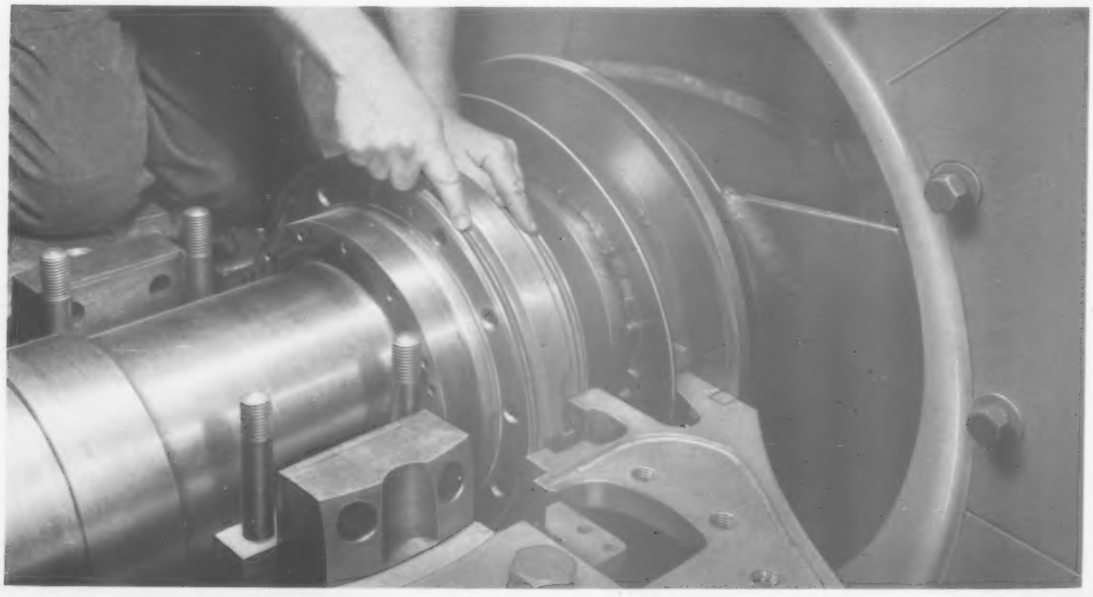

SEAL OIL at a pressure slightly higher than the hydrogen pressure is allowed to seep past the seal to prevent leakage of hydrogen to atmosphere.

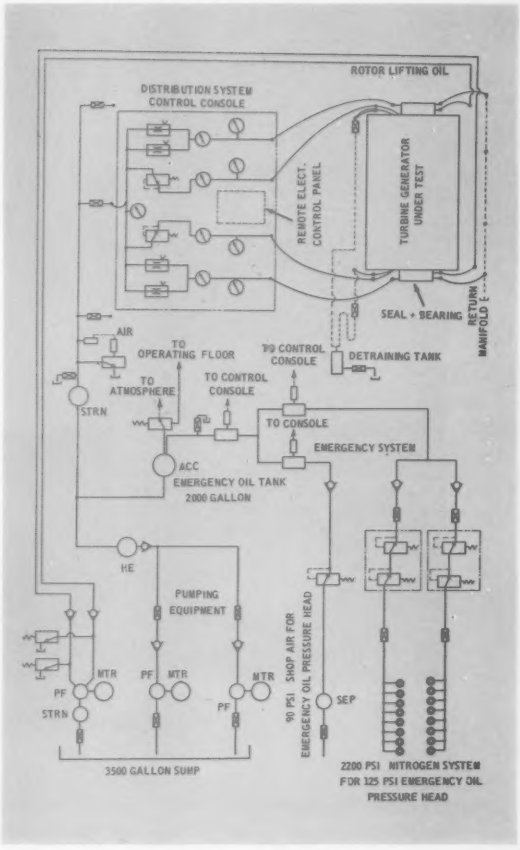

HYDRAULIC DEVICES in this schematic diagram are shown with recently adopted J.I.C. symbols. The diagram shows the complexity of the equipment needed to thoroughly test bearings and seals.

PUMPING SYSTEM, consisting of two 375-gpm low pressure pumps and a 5-gpm high pressure pump, supplies the oil for the bearings and seals of the machine being tested. A 2000-gallon emergency tank supplies bearing oil for a period long enough to shut down the machine if the normal oil supply fails for any reason.

MEZZANINE FLOOR of test pit is location for bearing and seal oil strainer, air-operated back pressure valve and hydrogen detraining tank. Hydrogen picked up by the seal oil is released in the detraining tank before the oil is returned to the sump.

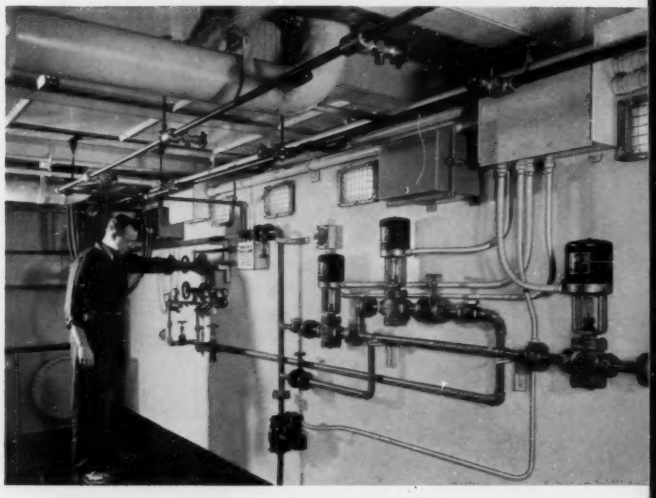

SHOP AIR and nitrogen supply manifolds used in conjunction with emergency oil supply are mounted overhead. Cylinders containing nitrogen are not shown. Nitrogen gas will be used when pressures higher than shop air pressure are needed for emergency shutdown.

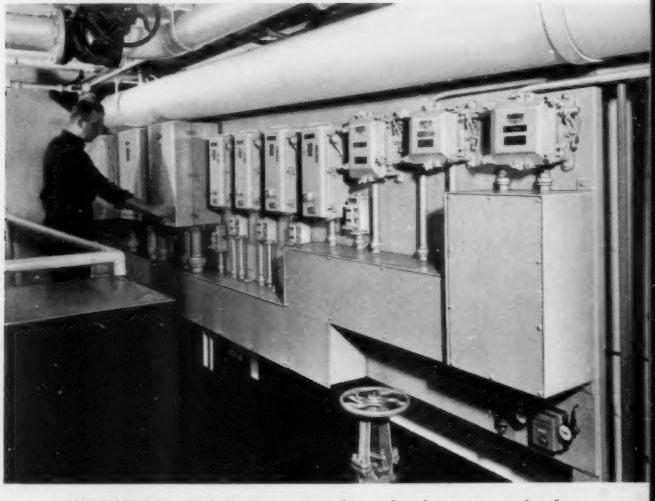

DISTRIBUTION PANEL has watertight enclosed starters and pilot devices because a water spray fire-protection system is used. Motors in pit operate on 480 volts, but control power is supplied by 480/110-volt control transformers in trough below the switches.

Regulators vs. Switched Capacitors

by **R. D. OKERBERG**
Transformer Department
Allis-Chalmers Mfg. Co.

Do regulators belong here and ca

SINCE FEEDER VOLTAGE REGULATORS or switched capacitors are the devices most likely to determine actual users' voltages, their proper application is a major factor in economic electrical power distribution.

Any corrective device must be inoperative within a certain region or "dead band" to prevent hunting or overcorrection. The size of this dead band, usually called band width, is a measure of the usefulness of the corrective device. The majority of feeder voltage regulators manufactured today have small ⅝ percent steps and accurate controls capable of maintaining voltages within plus or minus 1 percent of a predetermined value. The band widths of voltage controlled switched capacitors are usually considerably larger. To keep switching and control costs within economic limits, it is necessary to switch capacitors in relatively large increments. Band widths of 4 and 5 percent or greater result. Differences in band width can be evaluated by determining the amount of load or length of line which can be regulated.

Examining a section of a distribution system in which a certain tolerance has been set between the highest voltage allowable on the first distribution transformer and the lowest voltage allowable on the last distribution transformer may reveal a voltage profile similar to that shown in Figure 1. The band width in this case is shown as BW_1. Note that the sum of the band width (BW_1) and the voltage drop (I_1Z_1) must equal the voltage tolerance allowed (V max $-$ V min). Figure 2 shows the voltage profile of the same system but with a narrower band width (BW_2) and a larger voltage drop (I_2Z_2) so that the point of lowest allowable voltage is at the same distance as in Figure 1, where D_2 equals D_1.

How much more load can the system in Figure 2 carry?

Since the sum of the band width and voltage drop in

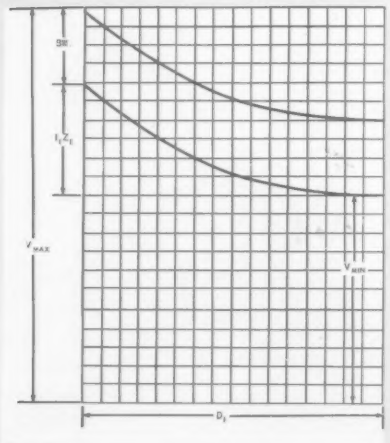

FIGURE 1

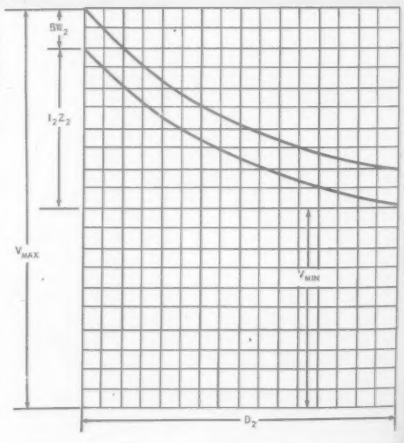

FIGURE 2

g here and capacitors here ?

each system must equal the voltage tolerance, the sums must be equal and can be equated.

$$BW_1 + I_1Z_1 = BW_2 + I_2Z_2$$

Since $D_1 = D_2$

then $Z_1 = Z_2$

and $$I_2 - I_1 = \frac{BW_1 - BW_2}{Z_1}$$

Also $$BW_1 + I_1Z_1 = V\ \text{max} - V\ \text{min}$$

Dividing the two equations:

$$\frac{I_2 - I_1}{I_1} = \frac{BW_1 - BW_2}{V\ \text{max} - V\ \text{min} - BW_1}$$

Multiplying by 100 to change to percent and putting the above into words we find:

$$\text{Percent load increase} = \frac{(\text{Original band width} - \text{New band width}) \times 100}{\text{Voltage tolerance} - \text{Original band width}}$$

To show how appreciable this can be, substitute some values in the above for a system with a 10 percent voltage tolerance when the band width is changed from 4 to 2 percent. The possible load increase equals $\frac{4-2}{10-4} \times 100$ or 33.3 percent. The curves of Figure 3 show the increased loads possible when band widths are reduced to 1¼ percent or two ⅝ percent steps.

Feeder loads may not always increase on a given feeder length as previously discussed, but may be increased by the extension of the feeder. Again this can be made possible by a narrower band width, although a different expression is needed for the amount of increase permissible. To determine how much D_2 can increase, let D_2 increase, picking up additional distributed load until the voltage reaches the minimum allowable V min.

In this case assuming equally distributed load, the current I_1 is proportional to the distance D_1 as is the impedance Z_1, so that the voltage drop I_1Z_1 is proportional to the distance D_1 squared. Likewise, the voltage drop I_2Z_2 is proportional to distance D_2 squared. We can then write:

$$\frac{D_2^2}{D_1^2} = \frac{I_2Z_2}{I_1Z_1} = \frac{V\ \text{max} - V\ \text{min} - BW_2}{V\ \text{max} - V\ \text{min} - BW_1}$$

$$\frac{D_2}{D_1} = \sqrt{\frac{V\ \text{max} - V\ \text{min} - BW_2}{V\ \text{max} - V\ \text{min} - BW_1}}$$

And subtracting 1 from both sides of the equation:

$$\frac{D_2 - D_1}{D_1} = \sqrt{\frac{V\ \text{max} - V\ \text{min} - BW_2}{V\ \text{max} - V\ \text{min} - BW_1}} - 1$$

Increase in feeder length

$$= \sqrt{\frac{\text{Voltage tolerance} - \text{New band width}}{\text{Voltage tolerance} - \text{Old band width}}} - 1$$

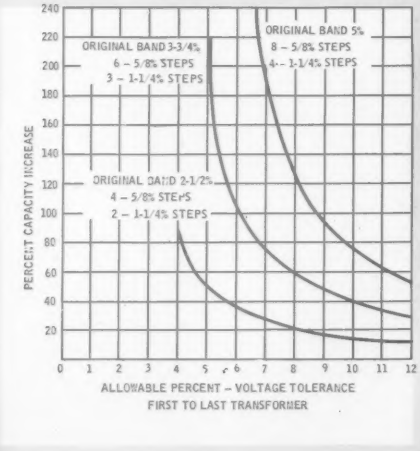

FIGURE 3

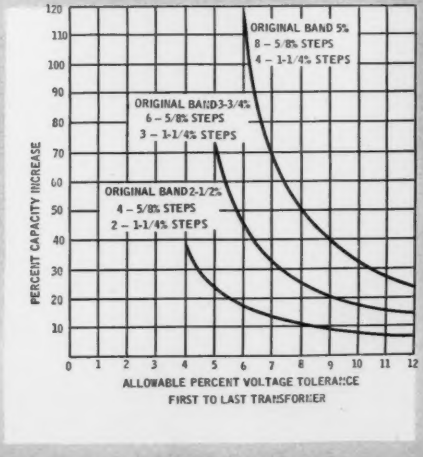

FIGURE 4

TABLE I

Equi-Cost Distances for 10 Percent Voltage Correction on Distribution Circuits with Voltage Regulators or Capacitors

Shorter distances favor regulators, longer distances favor capacitors

THREE-PHASE VOLTAGE	CIRCUIT KVA	EQUI-COST DISTANCE IN MILES	THREE-PHASE VOLTAGE	CIRCUIT KVA	EQUI-COST DISTANCE IN MILES
2500	500	1.4	7620	2000	4.0
2500	750	1.3	7620	2500	4.2
2500	1000	1.4	7620	3000	3.9
2500	1500	0.6	7620	3750	3.8
2500	2000	0.6	7620	5000	3.4
2500	2500	0.6	7620	6000	3.1
2500	3000	0.5	7620	7500	2.8
4330	750	2.7	8660	750	8.6
4330	1000	2.5	8660	1000	8.1
4330	1500	2.8	8660	1500	9.1
4330	2000	1.5	8660	2000	5.3
4330	2500	1.5	8660	2500	5.2
4330	3000	1.4	8660	3000	4.9
4330	3750	1.4	8660	3750	4.5
4330	5000	1.2	8660	5000	4.2
			8660	6000	3.9
5000	750	4.2	8660	7500	3.3
5000	1000	4.6			
5000	1500	2.0	12,470	750	14.6
5000	2000	1.8	12,470	1000	16.3
5000	2500	1.9	12,470	1500	14.8
5000	3000	1.9	12,470	2000	16.0
5000	3750	1.7	12,470	2500	16.9
5000	5000	1.6	12,470	3000	9.3
5000	6000	1.4	12,470	3750	10.3
			12,470	5000	9.2
7620	750	9.0			
7620	1000	7.7	12,470	6000	8.5
7620	1500	8.7	12,470	7500	7.7

The curves of Figure 4 show the possible increase in feeder lengths with additional distributed load when various band widths are reduced to two ⅝ percent steps.

A voltage regulator can only improve or correct voltage conditions at or beyond the regulator. Capacitors, on the other hand, by changing power factor and kva influence voltage conditions both before and after the point of installation. Figure 5 shows the full-load voltage profile of a uniformly loaded distribution feeder with a voltage regulator installed at the midpoint. Figure 6 shows the full-load voltage profile for the same feeder with voltage controlled capacitors installed at the midpoint. Whether the profile with the regulators or capacitors is better will depend to a large extent upon the respective band widths. Evaluation can be made between the band widths of the two methods by the formulas or Figures 3 and 4.

As mentioned before, the voltage change by capacitor control is effected by changes in the power factor and kva of the circuit. The majority of such installations have been on relatively low voltage high current feeders where changes in reactive drops can have a large effect. As distribution voltage increases and currents and conductor sizes decrease, however, changes in reactive drop become less and less effective.

The curves of Figure 7 show the relative voltage drops at various power factors for resistance to reactance ratios from 1:4 to 3:1. These curves are based on the real part of the voltage drop or $I\ (R\cos\theta + X\sin\theta)$ where R is the line resistance, X the line reactance, θ the power factor angle, and I the line current. The relative current has been taken as unity at unity power factor and proportionately increased at other power factors to maintain a constant kilowatt load.

Referring to Figure 7, curve *A*, for a resistance to reactance ratio of 1:4, which might be typical for a 2000-kva, 2400-volt feeder, changing the power factor from 0.70 lag to 0.95 lag changes the relative voltage drop from 5.2 to 2.3, a decrease of over 55 percent. For a feeder of the same kva at 12,000 volts the resistance to reactance ratio is slightly greater than 1:1; and from curve *D*, Figure 7, a change in power factor from 0.70 lag to 0.95 lag changes the relative voltage drop from 2.0 to 1.5, a decrease of only 20 percent. With resistance to reactance ratios as high as 3:1 (curve *G*), which may apply to laterals, taps, or branches of main feeders, changes in power factor have almost negligible effect in changing voltage drops.

The curves of Figure 7 have been extended to take in the range of leading power factors from unity to 0.60.

TABLE II

POINTS TO CONSIDER	MODERN REGULATOR	VOLTAGE-CONTROLLED SWITCHED CAPACITORS
Band width	Plus or minus 1 percent or less	5 percent or greater
Step size	5/8 percent	Usually several percent
Circuit power factor	Not important	Capacitors may cause leading power factor
Losses	Unchanged except for regulation losses	Probably reduced*
R:X ratio	Not important	May limit effectiveness of capacitors
Circuit demand	Unchanged	Probably reduced*

* Losses and circuit demand may be increased if power factor is made sufficiently leading.

While system stability usually prohibits leading power factors on generators, individual feeders may operate occasionally at leading power factors. It is interesting to note that for resistance to reactance ratios of 1:1 and greater, it is impossible to get voltage rises until the power factor becomes less than 0.70 leading.

The trend today is toward higher distribution voltages, a main reason being the smaller currents and hence smaller voltage drops for a given kva load. Because of the higher resistance to reactance ratios of such circuits, capacitor installations are considerably less effective.

As with any engineering decision, the final choice between regulators and switched capacitors is often a matter of dollars and cents. Direct comparisons can be made only for individual cases where all facts are known, but it is possible to reach some general conclusions. Since the amount of voltage change or correction by capacitors is determined by the amount of reactance through which the capacitor current flows, comparisons can be made on the basis of feeder length. Very short feeders require a number of capacitors, while longer feeders require fewer capacitors. Since the cost of a regulator is independent of feeder length, there is some point on the feeder where the cost of voltage regulation by capacitors equals the cost of regulation with regulators. For longer circuits capacitors would be less expensive, while shorter circuits favor regulators.

For such a comparison the following assumptions are made:

(a) Installed cost of capacitors $6.60 per kva.

(b) Substation transformer reactance 5 percent.

(c) Regulator cost for ± 10 percent to 5/8 percent step-regulators, single-phase distribution type or three-phase power regulators, plus $500 installation charge per single-phase unit and $1,000 per three-phase unit.

(d) Sufficient capacitors required to equal 10 percent raise of regulator (10 percent lower of regulator ignored).

(e) Conductor spacing 30 inches for 2500 and 4330 volts, 36 inches for other voltages.

(f) Substation transformers connected to an infinite bus.

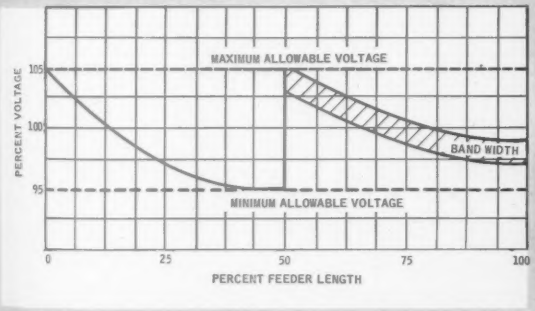

FIGURE 5

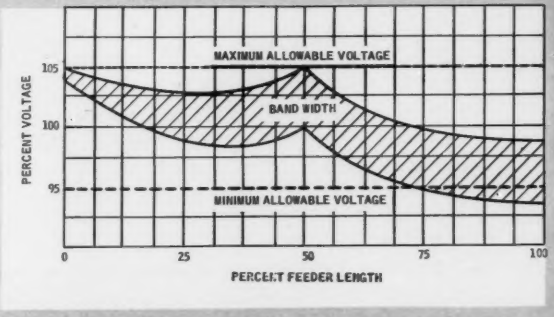

FIGURE 6

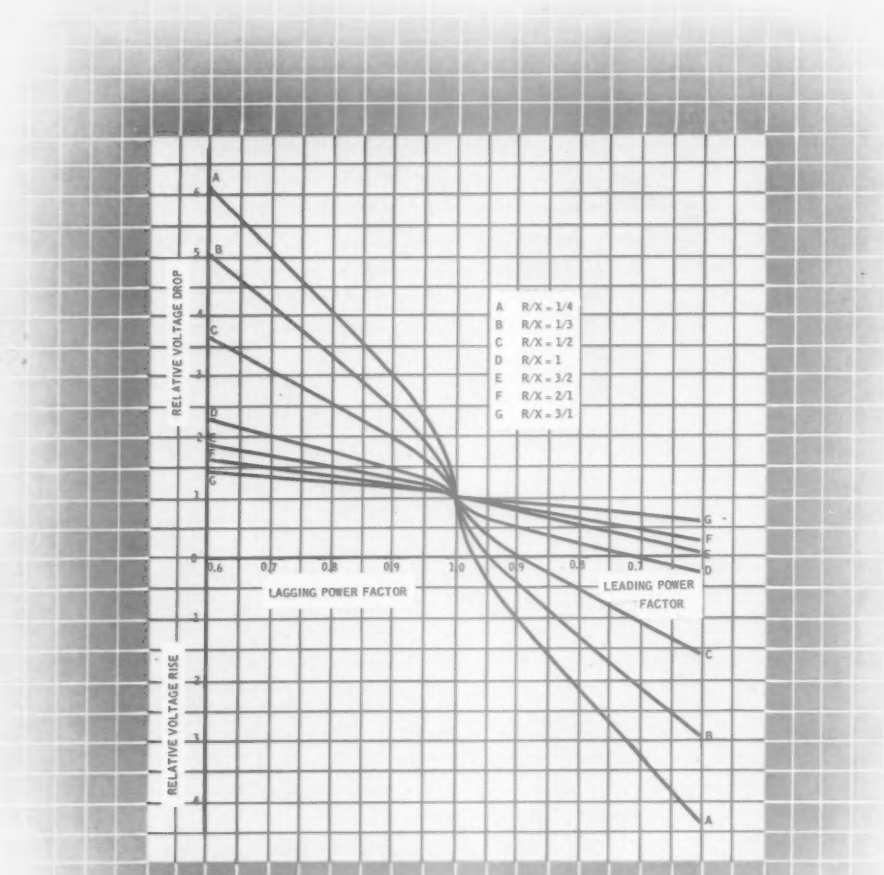

FIGURE 7

The results of this comparison are shown in Table I. As would be expected, the distances are greater for higher voltage circuits where the resistance to reactance ratios are greater.

Such a comparison, of necessity, ignores the capacitor advantage of reducing kva demand and conductor losses. In many cases, the kva of capacitors required is great enough to cause leading power factors which might not be acceptable. Since only half the regulator range had been used and band widths ignored, the comparison is felt to be a fair yardstick.

From the comparisons of Table I it is apparent that for substation regulation voltage regulators are more economical. For feeders of the listed lengths and longer, capacitors enter the picture. When a rough comparison shows initial costs to be about equal, the factors in Table II should be considered.

The final decision in many cases should be based on which is needed, voltage regulation or voltage improvement. There are some regulators which do nothing but raise the input voltage 10 percent continuously and are not really used as regulators. They probably could be replaced by capacitor installations just as well. On the other hand, many capacitor installations are used to improve voltages where regulation is actually needed. In some cases it may be best to use both capacitors and regulators, the capacitors being used to improve power factor and the general voltage condition and regulators to give close accurate control of voltage. This is sometimes done by turning the capacitors on when the regulator reaches its maximum raise position. The capacitors then remain on until the regulator reaches its maximum lower position. This is sometimes accomplished by using the limit switches in the regulator mechanism. Such installations gain the benefits of a reduced kva and losses possible with capacitors, and the narrow, accurate plus or minus 1-volt band width of modern voltage regulators.

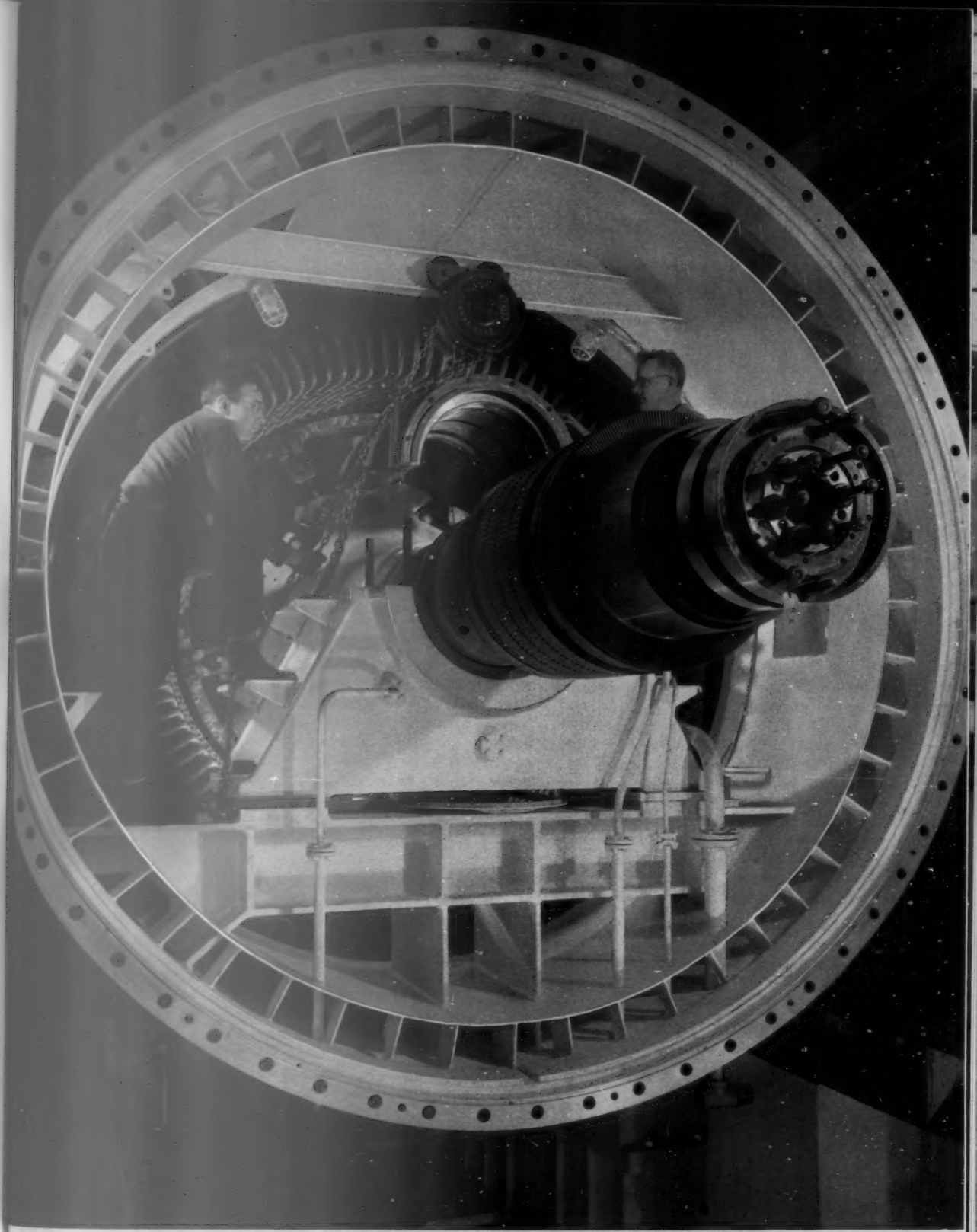

THIS HYDROGEN-COOLED SYNCHRONOUS CONDENSER will supply reactive kva to assure efficient use of power at a large processing plant having heavy induction motor loads. The overhung exciter armature and slip rings project into the exciter enclosure of this 50,000/21,000-kva 13,800-volt 720-rpm machine. Built-in rail and chain hoist make easy work of capping the massive bearing pedestals within the thick shell that seals hydrogen in — weather out.

AUXILIARY DRIVE MOTOR Keeps Pace with Modern Power

by **C. D. LAWTON**
Motor and Generator Section
Allis-Chalmers Mfg. Co.

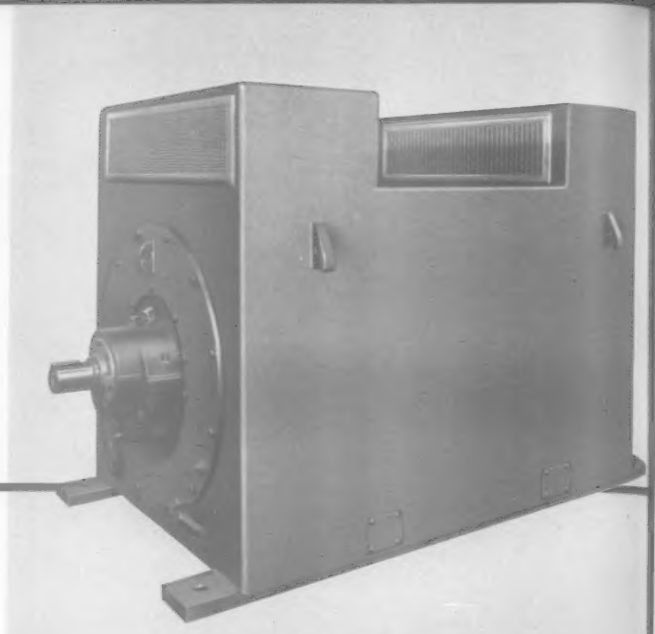

HOUSEKEEPING PRACTICES in power plants guided the location of air intakes and exhausts. **(FIGURE 1)**

Typifying the influence of power plant design and operating procedures on auxiliary drive motors is this new boiler feed pump motor.

ESTABLISHED TRENDS toward higher ratings, higher temperatures, and higher boiler pressures in modern generating stations have had their effect on power plant auxiliaries. As a result of these trends — and advanced thinking toward improved reliability — ease of operation, low sound levels, proper lubrication, minimum vibration, neat appearance, and convenience during installation and maintenance are design considerations that have acquired additional significance.

An example of how these trends are reflected in auxiliary motors is the completely redesigned, standard drip-proof, two-pole squirrel-cage induction motor shown in Figure 1. This motor incorporates many new features especially important for boiler feed pump and other services.

Some of the problems encountered in operating two-pole motors have centered around the bearings — primarily the result of oil leakage and vibration. While vibration has been effectively minimized as a trouble source by designing all 3600-rpm motors with critical speed safely removed from operating speed, a wide variety of bearing arrangements and seals have been applied with varying degrees of success.

Overlubrication can be a source of oil leakage. Too much oil floods motor bearings and breaks down the oil seals. For this new motor, the capsule-type bearing used so successfully on slower speed motors has been redesigned for high speed operation. This bearing, shown in Figure 2, assures adequate oiling without flooding or leakage.

Oil flow important

Lubricating oil is introduced into the bearings below the centerline. A small orifice in the incoming line, just inside the bearing housing, limits the flow of oil to approximately half a gallon per minute at about five pounds pressure. If higher pressures are necessary, this orifice helps maintain constant oil flow and prevents flooding.

After passing through the orifice, the oil flows into a relief at the side of the bearing, then spreads out along the bearing surface. About 80 to 85 percent drains into the oil reservoir before reaching the shoulders at the bearing ends. Oil slingers on the shaft and labyrinth seals on the bearing housing prevent oil from getting beyond the seals.

Oil vapors are sometimes present in the bearing housing between the bushing and the interior of the motor. The seals prevent these vapors from escaping. Sometimes, due to misadjustment when bearings are reassembled in the field, oil vapors may leak out of the housing. Anticipating this possibility, the bearing housing has been designed to provide atmospheric pressure relief so that oil vapors cannot progress farther into the machine. In addition, pressurized air from the motor's fan region is directed into a chamber around the shaft, passes through an annular seal into a second chamber, and vents to atmosphere. The constant flow of air positively prevents any oil vapors from getting beyond the atmosphere-vented chamber.

Differential pressures relieved

Although high speed motor bearings are designed for forced lubrication, oil rings are provided for emergency operation. The action of the oil rings can be observed

through sight ports. To insure that no oil vapor escapes, these ports are sealed with sight glass plugs for visual inspection. The bearing enclosure is vented to the atmosphere by a breather, similar to those used for automobile crank cases, located on the top side of the bearing. When attempting to pass through the breather, oil vapor condenses and accumulates in meshed copper, and eventually flows back into the bearing. No oil vapor can escape from the bearing enclosure.

Oil returns to the sump through a separate overflow compartment bolted onto the side of the bearing oil reservoir. Proper level is maintained by a weir, and the flow of oil is easily observed through a sight glass plug that permits looking down into the overflow compartment. When the motor is installed, an oil return line of large diameter is used to insure that overflow oil is carried away fast enough to prevent bearing flooding.

Sound level reduced

As 3600-rpm motors have increased in size to accommodate the greater load imposed by larger boiler feed pumps and higher pressures, noise has become an increasingly greater problem. It is recognized as a factor that reduces worker efficiency, and as a source of complaint where power plants are located near residential areas. Since the boiler feed pump motor has the highest sound level of all motors in a power plant, it is logical to reduce the sound level of this motor as much as possible.

Practically no magnetic noise is developed in a 3600-rpm squirrel-cage motor. Almost all noise is windage, the greater portion coming from the rotor fan. By reducing the noise at the point of generation, much lower sound levels can be accomplished. To reduce the amount of fan-generated noise, fans have been changed from axial flow propeller type to centrifugal type.

If air inlets are placed opposite the rotor fans, noise can come straight out into the motor room, and sound absorption is difficult to accomplish. To hold sound level down, the air inlets must be located away from the fans. A sectional view of this new motor, Figure 3, shows that fan-generated noise must follow a lengthy path of obstructions before reaching the air intakes. This long passage permits sound-deadening and sound-absorbing materials to be used where necessary. In addition, air baffles are of the spun type, and have no sharp-cornered joints or sections that can generate sound.

These design changes have resulted — depending upon motor size — in a noise level 6 to 10 decibles lower than possible with previous designs. Since a drop of three decibles means noise level is cut in half, the noise reduction has obviously been large.

Spiral ventilation cools motor

Air passages within the rotor and stator structures have also been modified to reduce windage noises and improve ventilation. The rotor is made up of circular keyed laminations mounted directly onto a forged shaft, and is a solid structure without ventilating ducts. The stator core, however, is designed for the circulation of air in a manner called "spiral ventilation."

Spiral ventilation has been used successfully on large steam turbine generators since 1937. In the spirally ventilated motor, that portion of the yoke behind the core is alternately divided into air intake and exhaust compartments. Depending on motor rating, from 8 to 12 intake and an equal number of exhaust compartments are used. See Figure 4.

Cooling air from the rotor fan passes across the stator coil ends before entering the air intake compartments. It is then directed through I-beam spaced vent ducts that

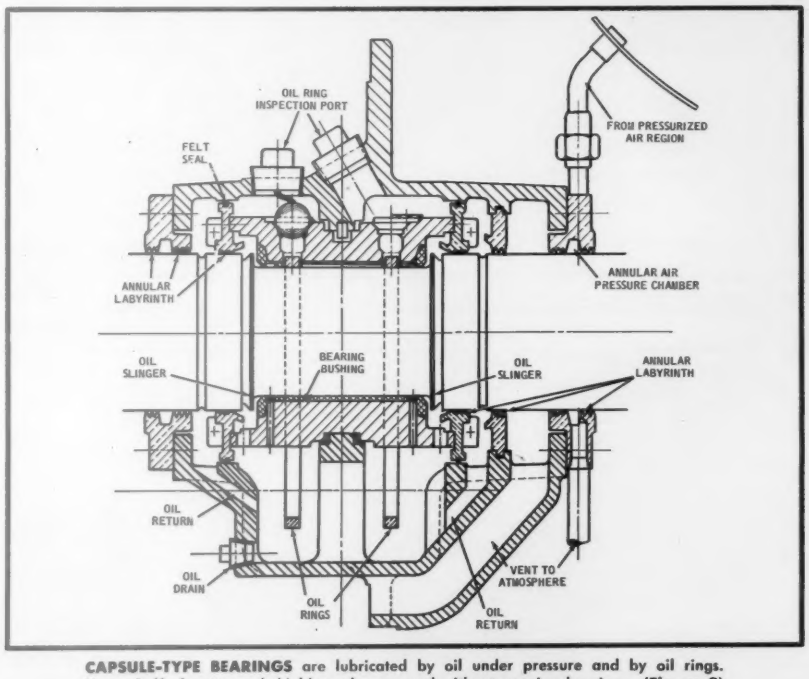

CAPSULE-TYPE BEARINGS are lubricated by oil under pressure and by oil rings. Upper half of motor end shield can be removed without opening bearing. **(Figure 2)**

divide the stator core laminations into a series of packets. Air passing through these spiral ducts cools the adjacent stator lamination packets and alternate groups of stator coils, then enters the air gap to absorb heat from the rotor before spiralling outward to the exhaust compartment. This type of ventilation also reduces noise.

Electrical parts are mechanically strong

The squirrel-cage winding has a very special and interesting design. The end rings are forged bronze to obtain a structurally strong material without flaws. Rotor rods are of oxygen-free high conductivity copper to prevent embrittlement while being silver brazed into the end rings. This is an extremely vital point in the design of these motors, and extra care and attention is given the end ring construction because cracking and breaking of brittle rod sections and end rings would be disastrous in service. On motors rated 2250 hp and larger, a steel retaining ring is placed over the entire end ring assembly, and a special steel balancing ring bolted on. Consequently, the rotor structure is not weakened mechanically by drilled holes necessary for balancing. See Figure 5.

Dewdrop-shaped rotor rods have the lip milled off at the ends to fit into round holes in the end rings. There is no open rotor rod slot section in the end ring assembly. Rotor rods cannot become loose, and once the silver brazing is finished, the end ring assembly is practically indestructible. The entire end ring structure is mounted on a spline and moves back and forth when heating and cooling.

Rotor rods have a drive fit in the rotor laminations, binding in the center of the rotor core. Because of this construction, all expansion is outward from the center, and distorted binding cannot occur in the squirrel-cage structure. A large retaining nut is screwed onto the shaft outside of each end ring assembly and tightened to secure the entire structure without binding or distorting the core.

Two classes of insulation used

Since boiler feed pump drives and other usual applications of large two-pole motors must be highly reliable, modified Class B insulating material is used for stator coils of motors rated 1250 hp and above to assure longer life. The slot portion has an outside layer of asbestos tape, hot pressed to slot size, to protect the coil structure against abrasion. Class A materials are used for the coil ends, and the joint between Class A and B insulations is accomplished by interleaving the materials over a 3-inch spread.

Class B material extends about an inch beyond the slots before any Class A materials are introduced. This is done because the coil end turns are located directly in the path of cool air coming from the fan, while the slot portion is subject to heating in the deep stator cores.

Cast brass brackets are used to brace the end turns on larger machines, while insulated brass rings are used for smaller ratings. Each coil is double laced and braced, and each coil side is laced to its adjacent coil side, with spacers placed between them. This method of lacing and bracing assures many years of service on installations employing full voltage starting.

Power plant practice influences design

Several design changes have been made which make this new two-pole squirrel-cage induction motor more consistent with modern power plant operating practice. For example, in housecleaning powerhouse basements, the usual location for boiler feed pump motors, floors are cleaned by playing water hoses directly on the floor. Water cannot splash into the air inlets of this new motor because

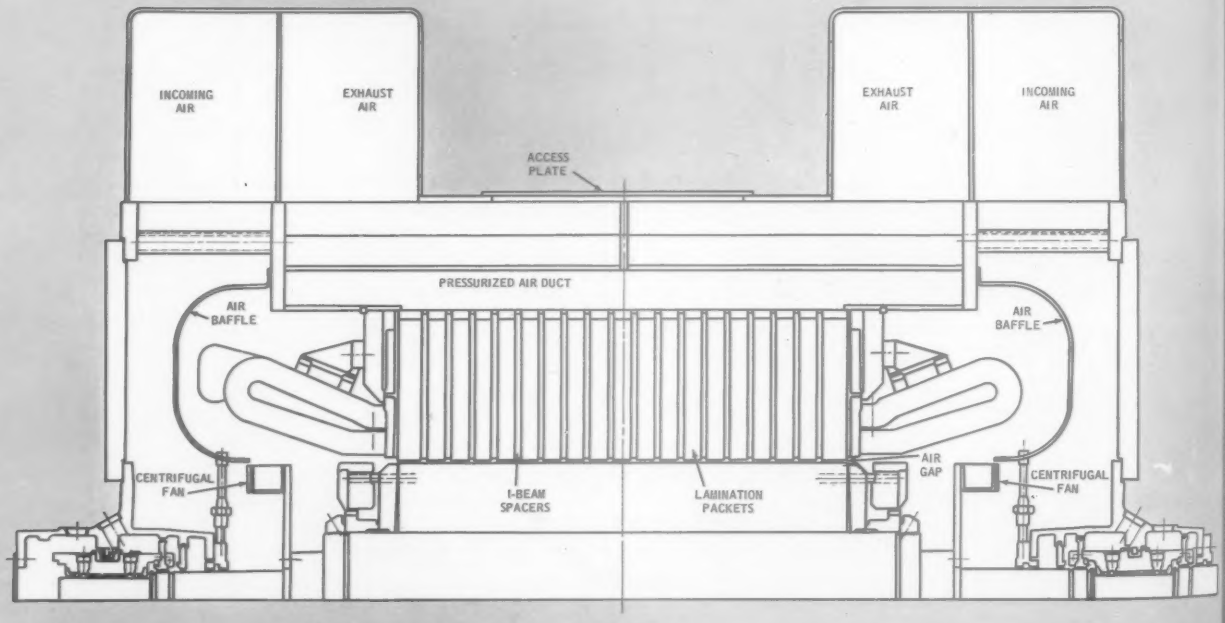

FIGURE 3

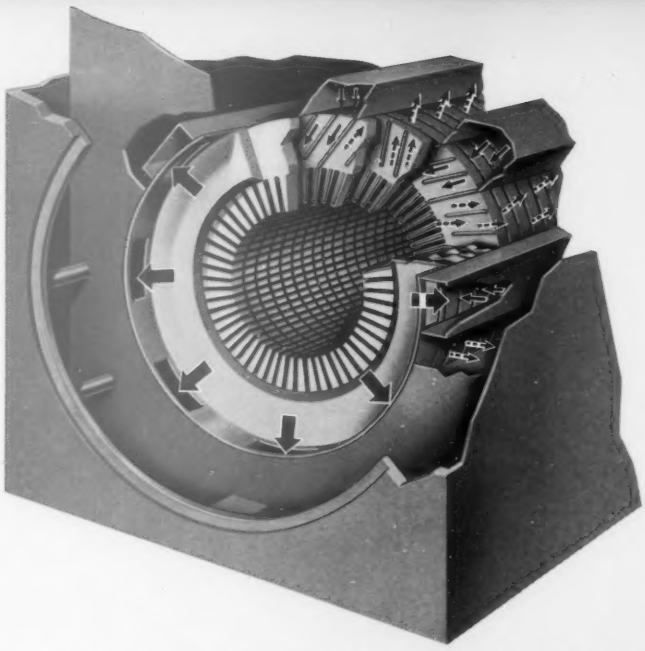

COOLING AIR from centrifugal fan enters air intake compartment openings, as shown by large arrows. These compartments become pressurized, forcing air (small solid arrows) through ducts formed between stator lamination packets by I-beams. Air then enters gap between stator and rotor and is exhausted through ducts, as shown by broken arrows. **(FIGURE 4)**

they are located on top of the machine and protected by drip or splash-proof grilles. Being off the floor, air intakes do not suck in dust and dirt. However, if the motor is to be placed in a consistently dirty location, intake grilles can be replaced with filters. The high location of air outlets prevents discharged air from blowing onto personnel. A steel plate all the way across the bottom protects the interior from water and dirt that might get in from underneath the yoke.

To simplify routine maintenance and inspection procedures, the upper half of bearing support plates can be removed for access to the interior of the motor without opening the bearings. Not only is there less mass to handle, but bearings that are operating properly can be left alone. This permits inspection and maintenance without exposing the interior of the bearing to dust and dirt usually in the air during periodic maintenance checks. The bearing end plates are thick sections of flat boiler plate steel and cannot wedge or bind the bearings when being bolted to the yokes.

In modern power plants, a great deal of attention is being given to the appearance of equipment. Consistent with this trend, this newly designed two-pole machine has smooth lines, devoid of appurtenances attached to the sides of motors. Even the attachment of stator lead terminal boxes to the outside of the motor is unnecessary. All leads, oil pipes, stator temperature detector terminal boards, and the like can be hidden. Access to them is gained through a plate on the side of the motor. There is more room for installation and maintenance with the leads arranged in this manner than if a terminal box is used.

Problems of installation, operation, and maintenance of auxiliary motors in modern power plants have all had a strong influence on this new machine. For example:

To insure successful operation, motors are balanced at the factory to within .001-inch vibration at operating speed.

Since it is usually desirable to have magnetic center located when motors are being installed, magnetic center is determined by measurement from the shaft shoulder to the bearing oil guard and indicated on an instruction plate attached to the bearing. This information is valuable when adjusting couplings and aligning machinery. Rotation plates relative to phase sequence and bearing insulation plates are furnished for convenience in installation and maintenance.

The requirements of modern power plant design and operating procedure have materially guided the design of this motor. Since 3600-rpm squirrel-cage motors are usually among the most important auxiliary drives in any plant, requiring the utmost in reliability and service continuity, careful attention has been given to design details that will assure many years of uninterrupted service. While these details apply to only one type motor, other types undergo the same engineering treatment to aid in the progress of modern industry.

CENTRIFUGAL FAN construction, bolted on balancing ring and retaining ring are visible on this 3000-hp motor rotor. **(FIG. 5)**

ALLIS-CHALMERS

SMOOTH AND LOW in silhouette — smooth in operation — this 75-mw, double-flow side-crossover tandem reheat turbine on the lines of Wisconsin Power and Light Company is the prototype of reheat units to 200 mw — all with supercharged hydrogen-cooled generators.

Ion Exchange— Electrochemistry's New Frontier

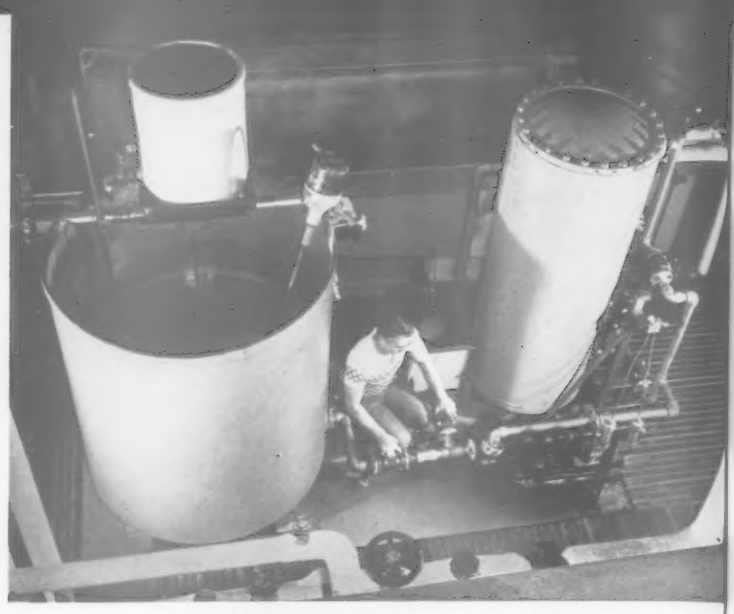

ION EXCHANGE EQUIPMENT installed at a midwestern industrial plant for purifying contaminated chromic acid anodizing solution.

by T. L. PANKEY
Engineer-in-Charge, Sales
Water Conditioning Section
Allis-Chalmers Mfg. Co.

Almost daily, industry is finding new and wider uses for these basic principles.

ION EXCHANGE is a chemist's term for a process that is to a great extent electrical in character. In this process, positively or negatively charged ions are exchanged to separate a substance from a solution.

Although this process is most familiarly known as an efficient and economical means of softening water for boiler make-up and domestic use, its applications are constantly being expanded. Metal platers, for example, use it to recover expensive metallic salts and to conserve water. Many other industries, especially those requiring completely demineralized water for steam and process use, are already using ion exchange and new applications are constantly being made.

Commercial installations of ion exchange equipment are based on the law of chemistry which states that nearly all acids, bases, and salts, when in solution, are disassociated into ions, which are atoms or groups of atoms carrying an electrical charge. Accordingly, ions of metallic elements have a positive charge and other elements a negative charge. Consequently, the former are called cations since they will migrate to a negatively charged plate or cathode and the latter are called anions since they are attracted to an anode.

Ion exchange principle explained

The ion exchange principle, used ever since ancient Greeks passed saline water through crushed rocks to make it potable, was not understood until the end of the last century. Then two English agricultural chemists, H. S. Thompson and J. T. Way, found that if certain soils were soaked in solutions of ammonium salts, the solutions lost ammonium and acquired calcium. They inferred that the calcium ions in the soil interchanged with the ammonia ions in solution.

This inference was based on the premise that the soil combined with ions having a positive charge and that only positively charged ions were interchanged. Thus, as the soil holding the calcium ions was saturated with an excess quantity of ammonium salt solution, positively charged ammonium ions would replace the calcium ions. As calcium ions were freed, they became a part of the solution.

Investigation of soils having the peculiar ability to trade ions was continued and chemists in Sweden discovered that a family of minerals — complex compounds of alumina, silica, and alkaline earths called zeolites or greensand — were especially capable of trading cations. However, no application was found for the discovery until after 1900, when a German, Robert Gans, softened water by passing it through zeolites.

He determined that the process removed calcium and magnesium ions responsible for hardness and replaced them with sodium ions until the supply of sodium ions held by the zeolite became exhausted. He also discovered that zeolites could be regenerated after they became exhausted by passing a sodium salt brine through them. Consequently, zeolite could be reused and the cycle repeated many times. This fact, he concluded, made the use of zeolite for water softening practical, since it eliminated handling large amounts of zeolites.

By 1930 this application was commercially exploited and widely used to soften water for boiler make-up, for domestic use, for commercial laundering and other processes.

Applications were limited because of the rather moderate capacity of natural zeolites. Also, natural zeolites are unstable at high temperatures or in highly acid or alkaline water.

SYNTHETIC ZEOLITE looks like sand, with each particle or bead a nearly perfect sphere. **(FIG. 1)**

Synthetic zeolites developed

Research to overcome the limitations of natural zeolites was begun in the 1930's, coincident with the development of new types of plastics. Efforts were directed toward developing plastic resins or synthetic zeolites that would have a greater capacity for exchanging ions while resisting oxidation and high temperatures. As a result of this research, many different high capacity resins for both cation and anion exchange were developed.

Accelerated research during World War II was centered around the sulfonic acid type exchange resin utilizing polystyrene as a base to form an insoluble cell or ionic grouping having large capacity for ion exchange. Experiments with these resins led to many of today's ion exchange applications. These resins, illustrated in Figure 1, made the treatment of electroplating wastes possible because they could resist oxidation by the acids.

Softening water with ion exchange

Ion exchange can be illustrated by using the domestic water softener operating on the sodium cycle as an example. The purpose of the process is to remove calcium and magnesium from the water, since they prevent the proper action of soap in the bath and laundry and form the crust in teakettles. The ion-exchange reaction is conducted in a container resembling a pressure filter.

Raw water, containing calcium and magnesium ions, flows slowly through the resin bed holding sodium ions. As water contacts the resin, calcium and magnesium ions are replaced by sodium ions from the resin and the effluent is soft water. This process is illustrated in Figure 2. When the resin bed approaches exhaustion its ion exchange ability falls off sharply, as indicated in Figure 3, and the process is stopped and the zeolite regenerated. After backwashing it to remove any suspended material and to loosen the resin bed, a strong solution of sodium chloride is passed through the resin bed, and sodium ions replace calcium and magnesium ions which form salts that are discharged to drain. Following this, the resin is rinsed, and is ready to begin the cycle again.

Water can be demineralized

Instead of using a sodium regenerated resin for the process, a resin charged with hydrogen ion may be used. In this case the resin is regenerated by passing a dilute solution of acid through it. This cycle, which produces an acid effluent, is paralleled with sodium zeolite softening to produce boiler feedwater of low alkalinity. The cycle, indicated in Figure 4, can also be used in conjunction with an anion exchange process to demineralize water. The process so thoroughly demineralizes water that it is, chemically, as pure as triple distilled water.

For the demineralization process, the effluent from the cation exchange unit is made to flow through an anion exchange bed. Consequently, positively charged ions are exchanged for hydrogen ions in the cation bed and the negatively charged ions are exchanged for hydroxyl ions in the anion bed. The final effluent is, therefore, pure water, since the hydrogen ion and the hydroxyl ion combine to form water. Upon exhaustion, the cation bed is regenerated with acid, either sulfuric or hydrochloric, and the anion bed is regenerated with soda ash or caustic soda.

Original applications of this process utilized "weak base" anion exchange resins and were limited because of

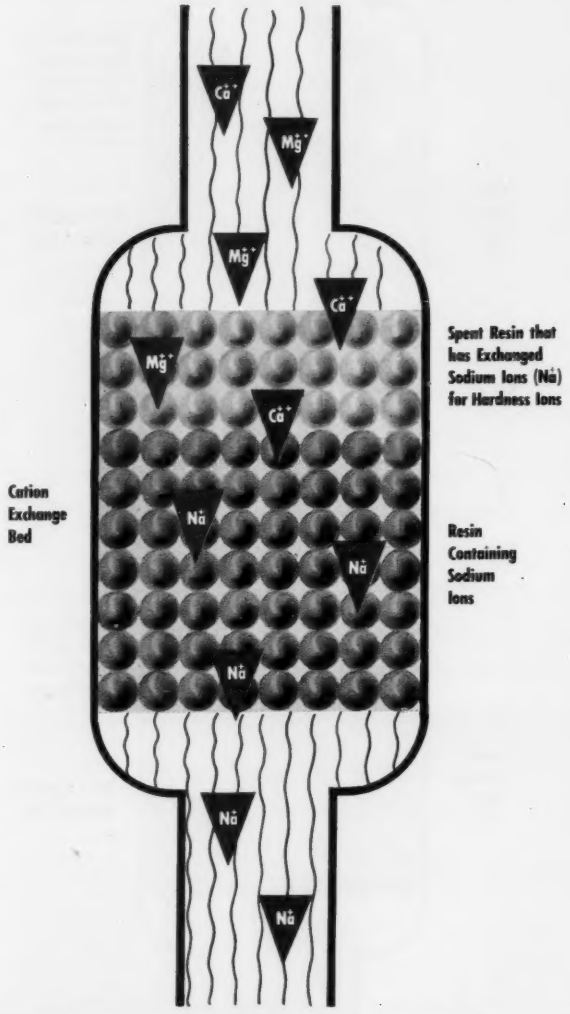

THE SODIUM ZEOLITE process is illustrated. **(FIGURE 2)**

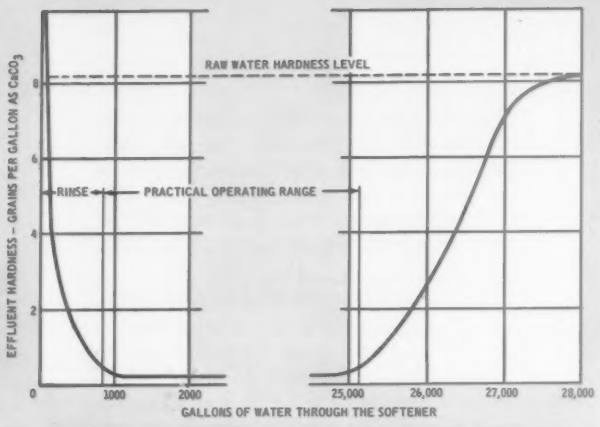

AN ION EXCHANGE BED loses its ability to exchange ions rapidly when it approaches exhaustion. **(FIGURE 3)**

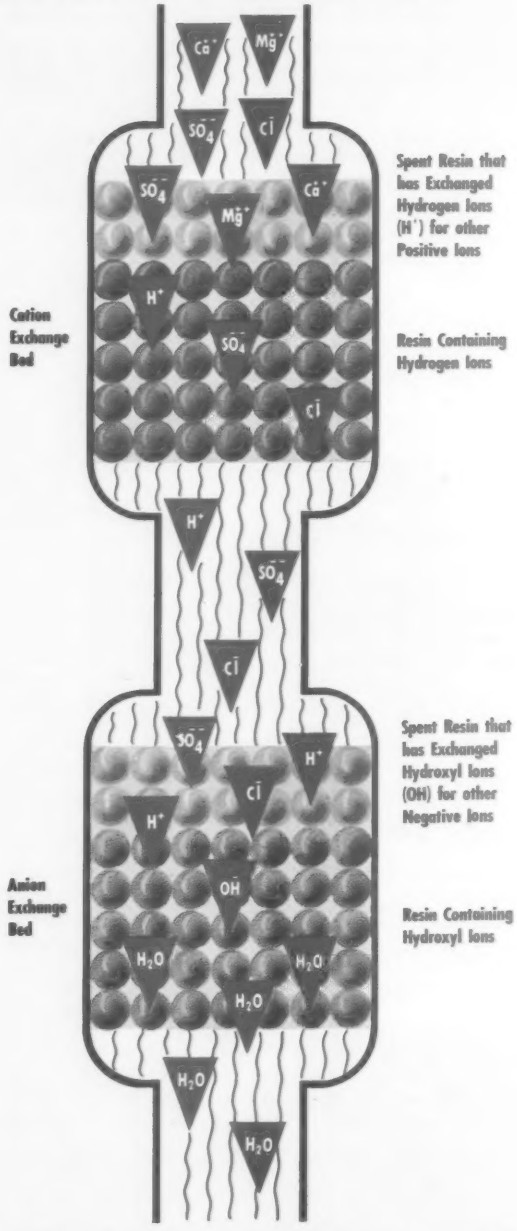
Spent Resin that has Exchanged Hydrogen Ions (H^+) for other Positive Ions
Cation Exchange Bed
Resin Containing Hydrogen Ions
Spent Resin that has Exchanged Hydroxyl Ions (OH^-) for other Negative Ions
Anion Exchange Bed
Resin Containing Hydroxyl Ions

ION EXCHANGE used for demineralizing water. **(FIGURE 4)**

inability of the resins to remove silica and carbon dioxide. Both are undesirable in boiler make-up water. Silica carries over in the steam and coats pipes and turbine blades with a hard glass-like deposit. Carbon dioxide is corrosive.

Development of a "strong base" type of anion exchange resin corrected that limitation, and now it is possible to remove all dissolved minerals, including silica, as well as carbon dioxide to values consistently as low as 0.1 part per million parts of water.

Industrial applications are widespread

With this demineralization process, raw waters of moderate salt content can be made chemically pure at a fraction of the cost of distilling water to identical purity. As a result, this process is used to supply pure water for industrial processes when the use of distilled water would be prohibitively expensive. See Figure 5.

For example, one manufacturer had difficulty obtaining an oxide film on aluminum parts that would resist corrosion when undergoing a severe salt spray test. Investigation showed that impurities in the anodizing rinse water prevented the film from making a uniform seal. Distilled water would have made this anodizing operation very expensive. Ion exchange to demineralize the rinse water was tried and proved completely successful. Not only was the rejection rate cut from near 70 percent to almost zero, but the rinse water was reused after removal of acid carry-over from the anodizing tank. Savings realized from this application amortized equipment costs in less than a year.

Applications of ion exchange resins to plating waste problems have been equally successful. One or more of four principal purposes are served by the application: (1) reduction of power requirements, (2) conservation of water, (3) reclamation of material, and (4) avoidance of stream pollution.

Improved product quality is one of the most important benefits of ion exchange when applied to plating operations such as anodizing and chrome plating.

Now under study is a method of using ion exchange to regenerate pickle acids used in the steel industry. When perfected, over a million tons of iron and great quantities of acid now lost each year will be recovered by this process.

Perhaps of even greater importance, with restrictions on water usage resulting from dire shortages in many communities, is the application of ion exchange to industrial waste problems to recover usable water.

Manufacturers have been forced to find ways of reducing water consumption in their plants. To solve the problem, plant engineers have investigated water uses to determine more efficient usage of water. These studies, in many cases, have indicated applications of ion exchange equipment which would provide means of treating water so that it could be reused. These applications also ease the load on sewage systems. An eastern manufacturer was able to save a large quantity of water by ion exchange purification of plating rinse water. Typical of this type of application is the use of ion exchange to reclaim chromic acid from an anodizing process, as shown in Figure 6.

Ion exchange has also been used successfully for separating and concentrating rare earth ores for atomic research and for isolating Thorium 230. The separation of these materials by this process is claimed to be the only practical means by which it could be accomplished.

A recent development in the field of ion exchange is the use of resin-impregnated membranes that can be used for separation of salts from solutions. Research on the application of these membranes is underway and one of the uses that shows promise is the treatment of sea water in large volumes so that it can be used for irrigation. A means of obtaining irrigation water from sea water is badly needed by farmers in many arid districts throughout the world.

Exactly what the future holds for these resins that trade ions is impossible to predict. Applications made so far may prove to be only a sampling of their commercial possibilities as the process of ion exchange becomes more widely understood.

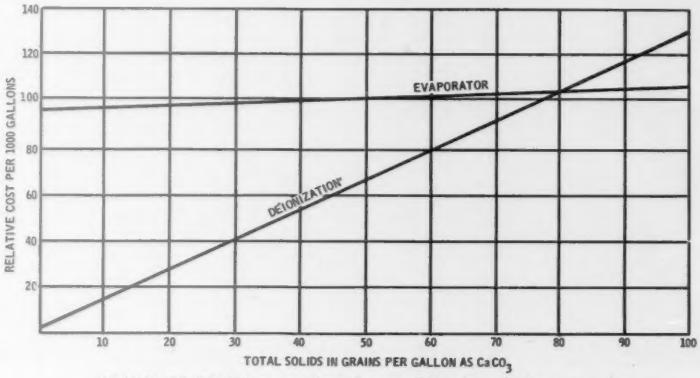

GRAINS OF SOLIDS per gallon of water determine whether ion exchange or distillation is the more economical way of purifying water. **(FIGURE 5)**

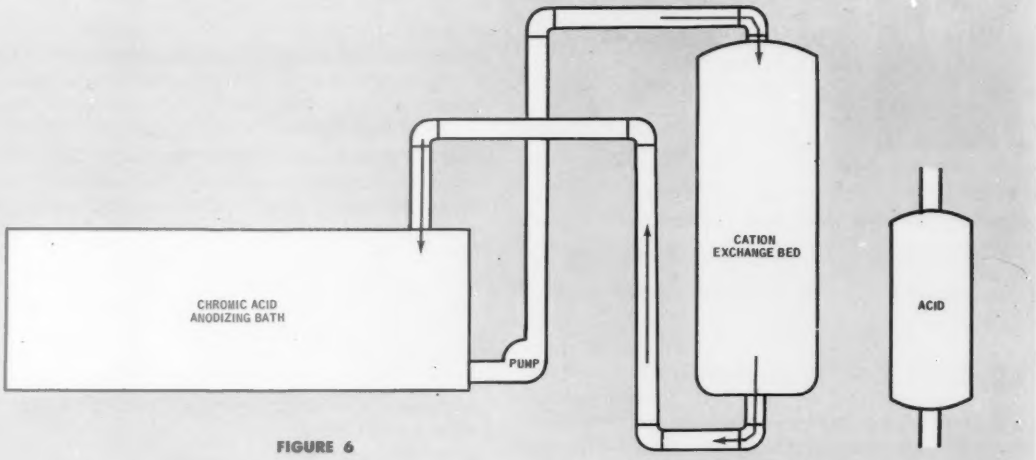

FIGURE 6

THE ABOVE DIAGRAM illustrates the arrangement of an ion exchange unit used to purify a chromic acid anodizing bath. The purpose of the equipment is to remove the aluminum transferred to the bath by the anodizing process.

In this process, aluminum parts are immersed in a chromic acid bath through which an electric current is passed. The aluminum becomes coated with an oxide film which is resistant to corrosion. During this process, some aluminum goes into solution in the chromic acid; this causes an uneven deposit of oxide film and the amount of electrical current required increases.

Contaminated chromic acid cannot be dumped to sewer, since it is highly toxic. Costly chemicals are frequently added to precipitate chromium for by-product recovery and to permit putting the water to sewer. This precipitation process is not economical in use of chromic acid nor does it maintain purity of the anodizing bath at a constant high level.

In the ion exchange process, the anodizing bath is regenerated by removing aluminum oxide which has been transferred to the bath. This is accomplished by pumping chromic acid from the anodizing tank through the cation exchange resin back to the anodizing tank. As liquor flows through the resin, aluminum ions are retained by the resin and hydrogen ions are released. The aluminum is reduced to a point where the liquor is as effective as a fresh solution.

The process may be arranged to purify the chromic acid on weekends or at night to prevent interference with regular production schedules. It may also be arranged for continuous purification with periodic regeneration of the resin.

Raw water is pumped through the resin from the bottom to the top to displace chromic acid and loosen the bed and is discharged to the anodizing tank. Following this, a solution of sulphuric acid is pumped from the dilute acid storage tank to the bottom of the exchange tank. It flows upward through the exchange material and out through the inlet system to discharge to waste. In flowing through the resin, hydrogen ions from the acid replace aluminum ions which were retained by the resin. As a result, the resin regains a charge of hydrogen ions and aluminum ions are discharged.

The next step is a rinse with raw water, from bottom to top, to waste, to flush the resin, leaving it in its original condition.

CORONA-FREE SWITCHGEAR

RADIO INTERFERENCE FILTER NETWORKS are not necessary in modern switchgear where all of the components have been carefully tested to eliminate corona interference.

by CARL E. MERCIER
Switchgear Dept.
Allis-Chalmers Mfg. Co.

Modern design and test techniques assure high dielectric strength and long insulation life in today's switchgear.

THERE ARE FOUR different types of high voltage tests used to assure high dielectric strength and insulation security in modern switchgear. These tests are 60-cycle corona, impulse, 60-cycle high potential, and radio noise. Corona testing is the most fascinating of these four tests.

Corona, which is an ionization of the dielectric material surrounding a conductor, occurs when the insulating material is overstressed by a high voltage. In switchgear the danger of corona is most likely to be found in the air adjacent to high voltage buses, bushings, and locations where small air gaps are present.

Corona can be very destructive because it produces oxygen in the free state and various nitrogen compounds which readily attack lead-covered cable, causing it to powderize into lead oxide and basic lead nitrates. Copper and silver are also attacked. This condition can be particularly serious on silver-plated contacts where corrosion can increase the contact resistance and cause excessive heating. Corona produces nitric and nitrous acid when moisture is present in the air. This acid condition not only causes corrosion of most metals, but also rapidly deteriorates insulation. High temperatures or hot spots developed by corona accelerate the aging of insulation, which in turn lowers dielectric strength. Corona, if present in switchgear, produces an undesirable high frequency signal which may travel long distances over transmission lines and interfere with radio, radar, and television reception. Since corona consists of random frequencies, it is very difficult to filter from transmission lines. The only method that can be used to eliminate this type of interference is to eliminate the source of corona. Extreme care is taken in the insulation of switchgear bus and other high potential components to eliminate corona. Figure 1 shows a shielded bus joint being assembled.

Corona eliminated

There are a number of methods that can be used to eliminate corona:

1. Increase spacing.
2. Improve geometric configuration.
3. Provide shielding.
4. Improve voltage distribution.
5. Eliminate air gaps, either electrically or mechanically.

Since corona in air is an ionization of the air caused by a voltage high enough to exceed the critical gradient of the air gap, the first logical step in eliminating corona is to increase this air gap. The air gap size for a required

corona level depends on the geometric configuration. The curves of Figures 2, 3, 4, and 5 show the effects of spacing for four basic configurations with relation to a plane: a plane, a sphere, a corner, and a cylinder.

Since space requirements often make it impossible to increase the size of the air gap, design engineers find it necessary to resort to other methods of decreasing the stress. One method, a change in geometric configuration of the device, has an important effect on the voltage stress across an air gap. Data taken from the curves of Figures 2, 3, 4, and 5 show the effect of geometry on a 1-inch air gap.

The data in Table I show the effectiveness of changing the geometric configuration.

In many cases, minor configuration revisions will result in a major improvement in corona level. Generally, it is good design practice to round off sharp corners on conductors that might undergo high voltage stress. Figure 6 shows how an insultor was redesigned to raise the corona level by improving the terminal geometry.

Another method used to eliminate corona is by applying shields around conductors that have high stress points. Since it is usually cheaper to resort to geometry correction, shielding is not used too often. However, there are some economical applications of a shield on a high voltage bus bar T-joint. The shield is placed over the hardware in order to eliminate the high stress points at the threads and corners on the hardware. The shield is used in conjunction with a high dielectric strength insulating boot. Figure 7 shows the effectiveness of the corona shield on a bus bar T-joint. The shield raises the corona level from 23 kv to 36 kv for a 1-inch spacing.

Dielectric constant is key to corona

Usually, complicated configurations can be broken down into an equivalent circuit. The equivalent circuit of an

NEOPRENE BOOT with metal shield greatly simplifies bus installation or changes, and provides a high corona level for 1200 and 2000-amp, 5000-volt bus joints. **(FIGURE 1)**

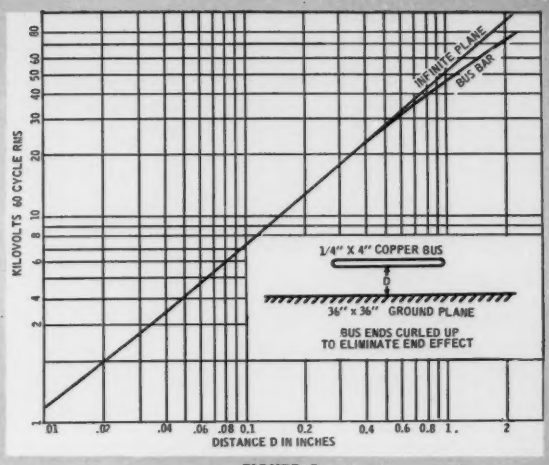

FIGURE 2

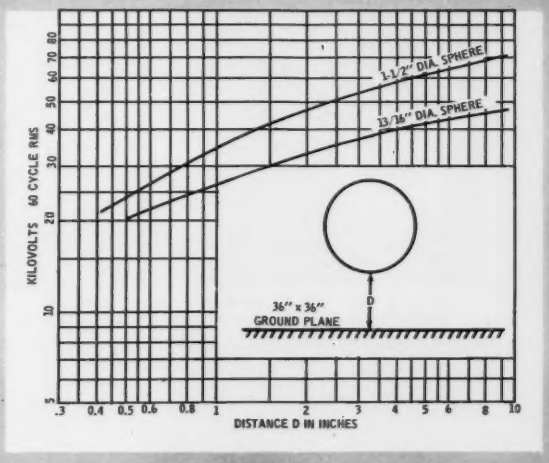

FIGURE 3

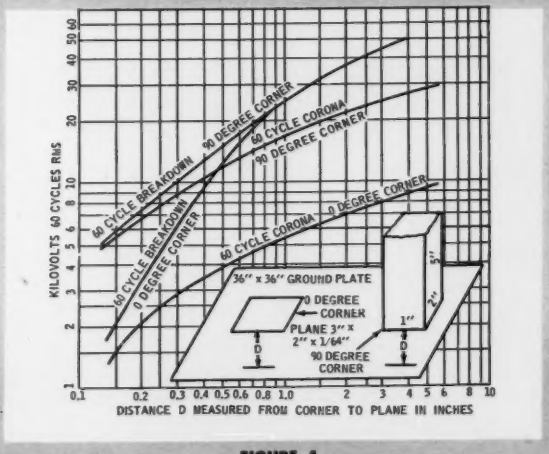

FIGURE 4

TABLE I	
Geometry	Kv Corona Voltage with 1-inch Air Gap
0° Corner	5.4
90° Corner	17
13/16" Dia. Sphere	26
1½" Dia. Sphere	35
½" Dia. Cylinder	35
1" Dia. Cylinder	42
Plane	51

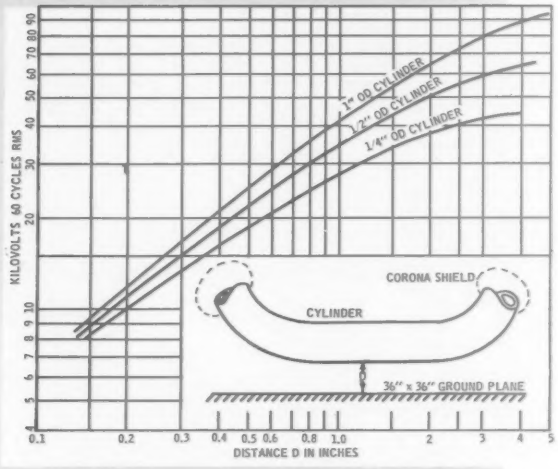

FIGURE 5

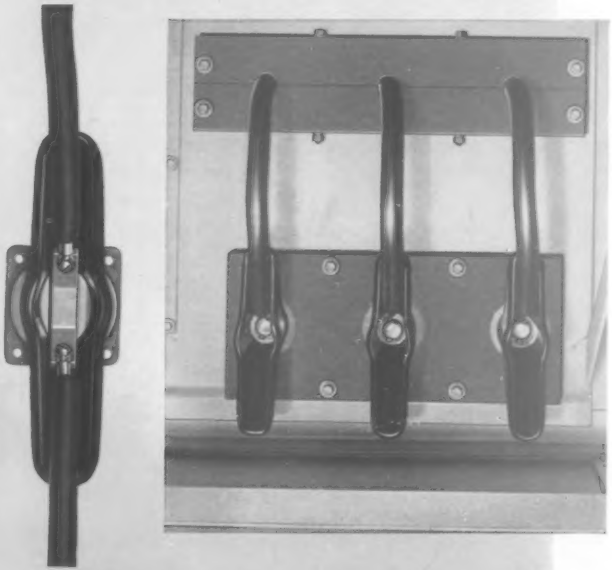

FUSE CONTACT GEOMETRY, left, was changed to the smooth rounded terminal, right, to eliminate corona at this point. Corona here might cause contact deterioration. **(FIGURE 6)**

insulated conductor could be a simple series capacitance circuit. Since the dielectric constant is known for the insulation being used, it is easy to calculate the impedance of each capacitor. The voltage distribution across each capacitor can be calculated as a series circuit.

The dielectric constant of the insulation in series with an air gap determines the voltage distribution. For a given air gap in series with a solid insulation, it is preferable to choose an insulation with a low dielectric constant so that the stress on the air would be minimum.

Since corona occurs when air is overstressed, it is possible to eliminate this corona by eliminating the air gap either electrically or mechanically. In eliminating an air gap electrically, both surfaces bordering the air gap may be coated with a conducting or metalized paint, or metal foil. The two conducting surfaces are then tied together electrically to eliminate the voltage across the air gap. The air gap can be eliminated mechanically with a filler, such as transformer oil, resin, or petrolatum.

Corona is detected and located

Five different methods can be used for corona testing: oscilloscope, audible, visual, radio noise, and Schering bridge.

The oscilloscope method of detection of corona is the most sensitive of the five methods. A corona setup that can be used with the oscilloscope is shown in Figure 8. The operation of the circuit is very simple. The low voltage side of the potential transformer is excited with a variable voltage from a 60-cycle source. The device under test is connected directly to the ungrounded side of the high voltage winding of the potential transformer. The device is placed in series with radio-frequency pickup coil L_1 and a current-limiting resistor R_2. A radio-frequency bypass capacitor is placed across the high voltage winding, acting as a short circuit to corona frequencies. The coupling to the high sensitive oscilloscope is through the small capacitor C_1. This capacitor is used to block out part of the 60-cycle charging current to the oscilloscope. A spark gap is used to protect the operator and the oscilloscope from high voltages that would be developed across the oscilloscope if pickup coil L_1 opens or fails, or if the test device should fail. This capacitor C_2 can be very valuable in checking the exact source of corona. Since the potential transformer can act as a voltage amplifier for any interference occurring on the low voltage side, it is possible to feed corona from the power line into the measuring circuit. The transformer bypass capacitor C_2 shorts out this interference and prevents it from feeding into the oscilloscope.

A check with the oscilloscope can easily be made in order to check the corona source. When the corona signal appears on the oscilloscope and its amplitude decreases when the bypass capacitor C_2 is removed, then corona is due to the device under test. If corona amplitude increases, the corona signal is being fed through the transformer. The 60-cycle filter capacitor C_1 is used to prevent overloading of the oscilloscope. It is, however, very valuable to have a small amount of 60-cycle signal feeding into the oscilloscope, because it can be used as another check on corona location.

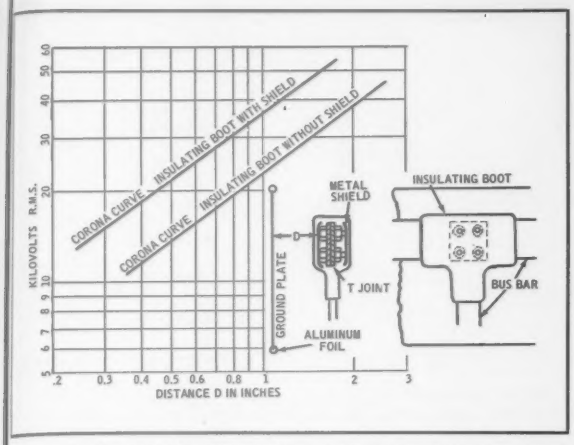

METAL CORONA SHIELD, shown in Figure 1, added 13 kv to the corona level of the insulating boot without the shield. **(FIGURE 7)**

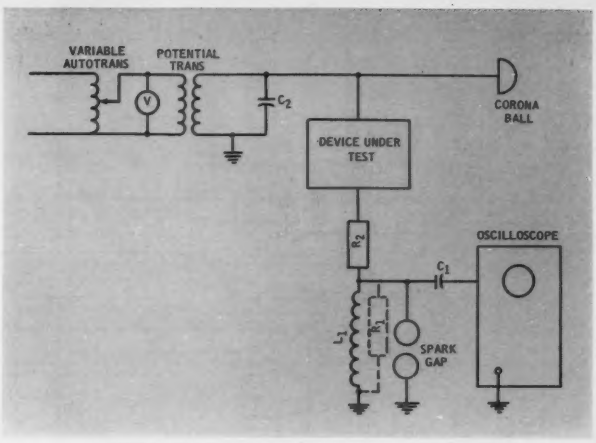

OSCILLOSCOPE METHOD is the most sensitive means of detecting and locating corona in switchgear. **(FIGURE 8)**

As an example, if the corona is external or internal with respect to the test set-up, corona that is developed by the device under test would be initiated by either the positive or negative peaks of the 60-cycle wave form. Corona that is external to the test may not have any synchronization with the test voltage. At times, depending on the capacity of the test device, it may be necessary to use a more elaborate 60-cycle π filter in order to increase the sensitivity of the pickup circuit. The 60-cycle signal can thus be almost entirely eliminated from entering the oscilloscope.

In running switchgear corona tests where it is important to study the corona characteristics, the radio-frequency pickup coil L_1 is replaced with a resistor R_1. The corona then appears as a rectified pulse instead of pulse oscillations as with a pickup coil. The rectified corona current is more sensitive to voltage changes than the pulse oscillations and enables the test operator to determine on what voltage peak the corona is initiated or is predominant. By comparing the test data with known corona characteristics, it appears that the corona can be classified as being internal or external. It has also been observed that corona occurring at a conductor appears as large surges, usually several times the amplitude of that of the nonconductor. There is, however, one distinct advantage in using the radio pickup coil in place of the resistor: the pickup coil increases the ratio of corona current to 60-cycle charging current. This enables the test operator to take full advantage of the amplification of the oscilloscope. Figures 9, 10, and 11 show corona characteristics as obtained with resistor or r-f pickup coil.

Corona hiss is warning

Audible corona can be detected in a low noise level room. The test setup is similar to Figure 8, except that now the spark gap is shorted out, thus eliminating the pickup coil and the oscilloscope. The voltage input to the transformer is raised by the operator until corona is heard by the test engineer. The simplest method of "hearing" corona is through the use of a 2-inch diameter phenolic tube of a length proportional to the test voltage. However, due to the high voltage, this method requires caution on the part of the test engineer. Checking for audible corona can be very valuable to the test engineer as a double check on the oscilloscope method of locating corona.

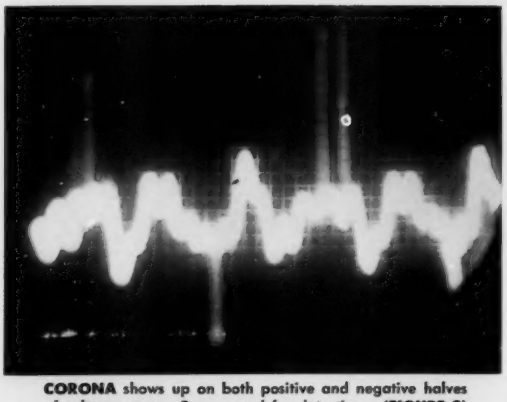

CORONA shows up on both positive and negative halves of voltage wave. R_1 was used for detection. **(FIGURE 9)**

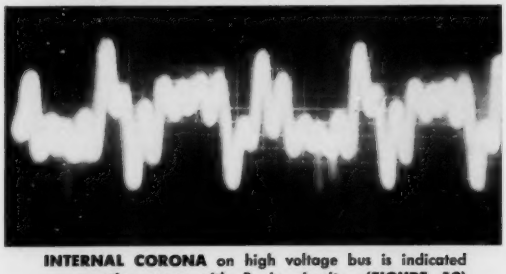

INTERNAL CORONA on high voltage bus is indicated on negative wave with R_1 in circuit. **(FIGURE 10)**

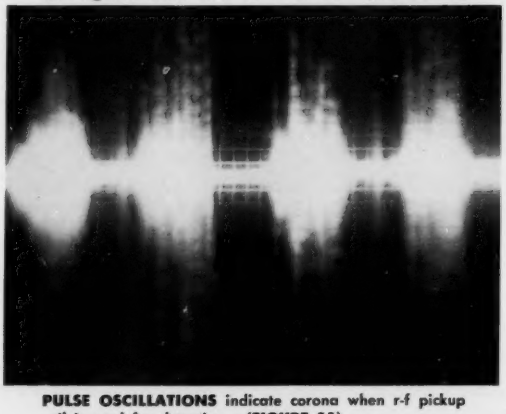

PULSE OSCILLATIONS indicate corona when r-f pickup coil is used for detection. **(FIGURE 11)**

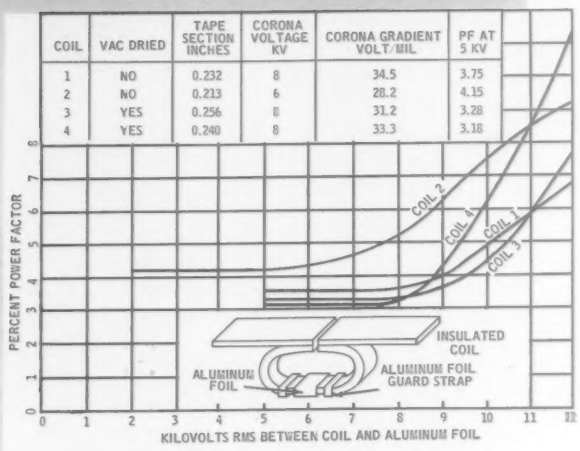
COIL | VAC DRIED | TAPE SECTION INCHES | CORONA VOLTAGE KV | CORONA GRADIENT VOLT/MIL | PF AT 5 KV
1 | NO | 0.232 | 8 | 34.5 | 3.75
2 | NO | 0.213 | 6 | 28.2 | 4.15
3 | YES | 0.256 | 8 | 31.2 | 3.28
4 | YES | 0.240 | 8 | 33.3 | 3.18
PERCENT POWER FACTOR
COIL 2
COIL 4
COIL 1
COIL 3
INSULATED COIL
ALUMINUM FOIL
ALUMINUM FOIL GUARD STRAP
KILOVOLTS RMS BETWEEN COIL AND ALUMINUM FOIL

FIGURE 12

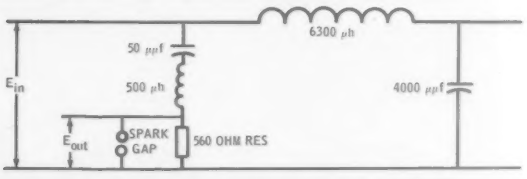

RADIO NOISE TEST CIRCUIT resonates at 1 megacycle, as is shown below. Variations in spark gap have no effect on frequency response of the circuit. **(FIGURE 13)**

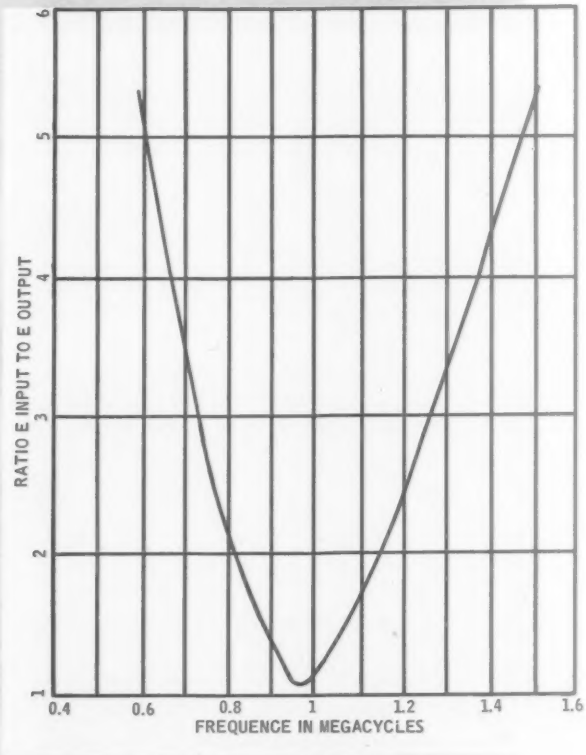

FIGURE 14

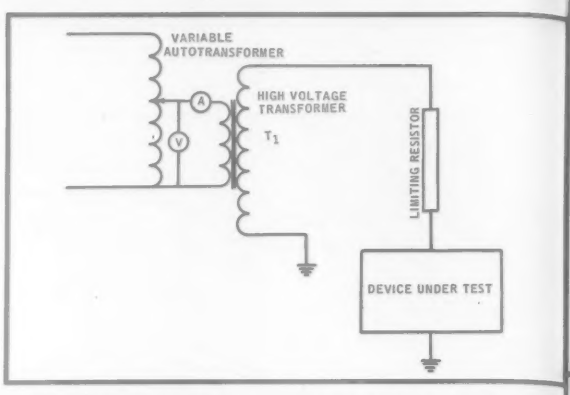

HIGH POTENTIAL TESTS prove quality of the total insulation between conductors and between conductors and ground. **(FIG. 15)**

Corona can also be detected visually by running tests in a darkened room. This method is good for external corona detection only and is not generally used because of its limitations.

The Schering bridge method of detection of corona can be very accurate on small samples. The Schering bridge is a simple device used for measuring the power factor of an insulated specimen. The power factor of a specimen remains constant below the corona voltage, but as soon as corona is developed, the corona loss increases the power factor. The corona voltage can be determined very accurately by plotting a curve of power factor versus voltage. The point at which the power factor curve breaks off from a straight line represents the corona voltage, or minimum corona level.

On large specimens, where the corona loss may be an insignificant percentage of the total loss, the Schering method is not sufficiently accurate. Figure 12 is a power factor test on an insulated coil to indicate corona level.

Radio interference checked

Radio noise tests are run on switchgear to measure the amount of corona present at the radio frequencies. The present switchgear standards establish interference limits in microvolts at one megacycle. The circuit used to measure radio noise is shown in Figure 13. The high voltage is applied to the switchgear through a high voltage transformer. A 6300-microhenry choke coil is placed between the switchgear and high voltage transformer in order to prevent corona from being fed into the noise meter from the source of high voltage. A 4000-micromicrofarad capacitor is used in conjunction with the 6300-microhenry choke in order to short out corona feeding in from the source. The series circuit, consisting of the 50-micromicrofarad capacitor and the 500-microhenry coil, has two purposes. The capacitor acts as a 60-cycle block to the line frequency, thus eliminating a 60-cycle signal from the noise meter circuit. The 60-cycle frequency itself is not harmful to the noise meter, but the voltage might be of such an amplitude that it would burn out the meter. The series arrangement also provides for selectivity. This combination is resonated at one megacycle.

The frequency response curve of this circuit is shown in Figure 14. When this series resonant circuit is excited with a 1-megacycle corona signal, the impedance of the series tuned circuit is very low and almost all the corona

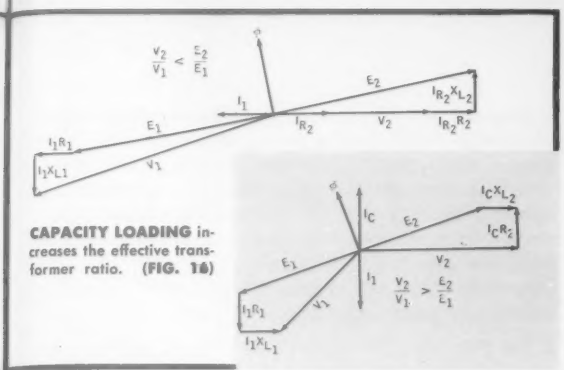

CAPACITY LOADING increases the effective transformer ratio. **(FIG. 16)**

RESISTANCE LOADING decreases the effective transformer ratio. Excitation current is neglected in these vectors. **(FIGURE 17)**

voltage developed in the switchgear is applied across the radio noise meter. This circuit has an efficiency of 88 percent at one megacycle. The 560-ohm carbon resistor is merely a load resistor for the radio noise meter. The radio noise meter is a special high frequency receiver. It has a specific gain and band pass as specified by switchgear standards. The circuit is battery operated and well shielded in order to keep the interference feeding into the set at a minimum. The radio noise meter has a microvolt scale which can be calibrated with its own internal oscillator.

For greatest accuracy radio noise tests should be operated in a shielded room in order to avoid erroneous pickup. Since radio noise is usually a direct product of corona, any scheme used to eliminate corona will eliminate radio noise. A radio noise test indicates the amount of corona voltage present at a given frequency but is not sensitive to various frequency combinations and cannot be used to locate corona.

High potential test proves design

High potential 60-cycle testing is another phase of testing switchgear equipment. This test differs from corona testing in that corona testing is merely a test of air gap dielectric strength, whereas high potential testing is to a greater degree a dielectric strength test of the solid insulation. Normally, considerable care is employed in eliminating high voltage stresses in and adjacent to the insulation where thermal and eventual electrical breakdown might occur; but in high potential breakdown testing, the high dielectric strength of the insulation is more essential than the factors generally considered important in maintaining a high corona level.

Switchgear potential test values are standardized. These standards specify that switchgear equipment must withstand a high potential test voltage for one minute at its rated test voltage. A typical test setup is shown in Figure 15. T_1 is a high voltage transformer and is excited on the low voltage side from a variable voltage source. Resistor R is used in series with the test specimen in order to limit short circuit currents in the high voltage winding. An ammeter placed in series with the low voltage winding is important to the test engineer, because the amount of current being consumed is a good indication of the condition of a test specimen during high voltage application. The voltage on the high side of the transformer is very difficult to measure without expensive meters; therefore,

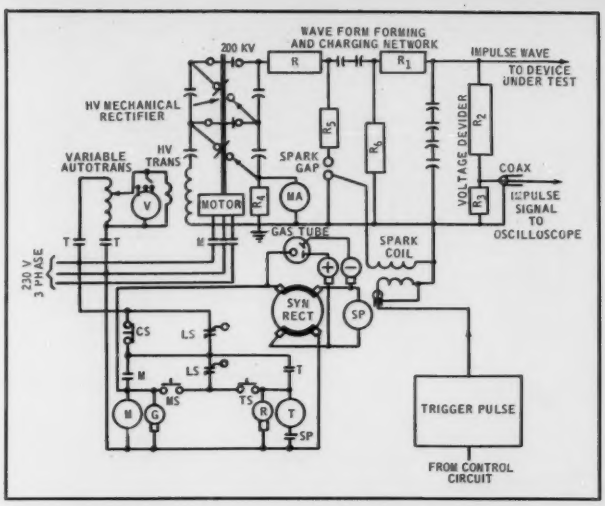

DESIRED VOLTAGE and wave shape for impulse testing of switchgear is obtained with circuit. **(FIGURE 18)**

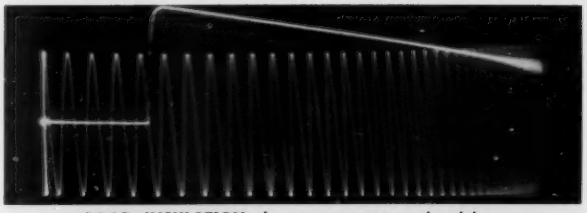

GOOD INSULATION shows no corona or breakdown on impulse oscillographic test. **(FIGURE 19)**

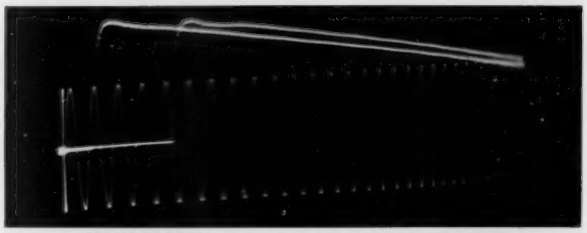

OSCILLOGRAPH shows corona is present on these two impulse waves and correction must be made. **(FIGURE 20)**

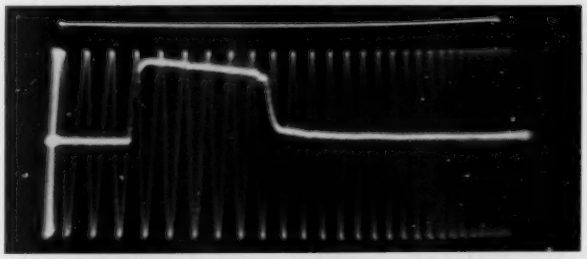

IMPULSE FAILURE of poor insulation to ground is shown on oscillographic test. **(FIGURE 21)**

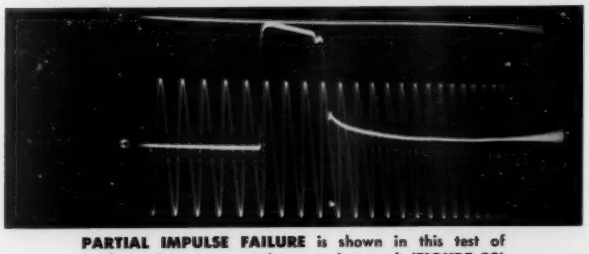

PARTIAL IMPULSE FAILURE is shown in this test of insulation between a conductor and ground. **(FIGURE 22)**

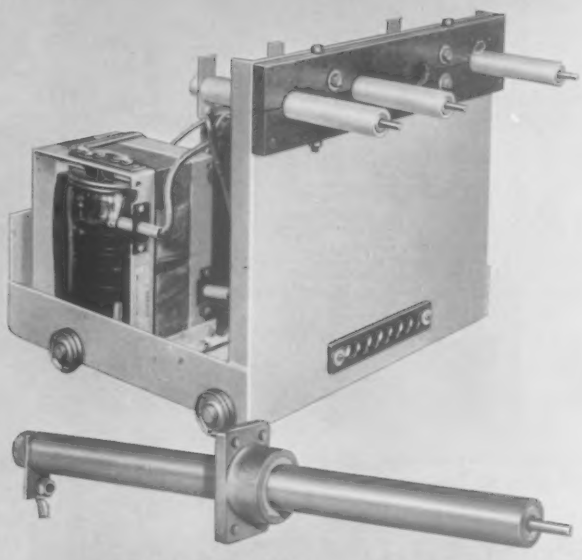

INCREASED CORONA LEVEL was obtained through the use of increased spacing to ground. Fuse holder mounting ring was replaced with an insulated mounting clamp.

CORONA between the bus and its insulating sleeve was eliminated electrically by coating the inside surface of the sleeve with a semi-conducting material.

SOLID INSULATION was used to eliminate the air gap between the coil insulation and grounded frame of this new design of current transformer rated 15 kv.

in most test setups it is very convenient to calibrate the circuit with a voltmeter in the primary side of the transformer. Calibration is done with a spark gap voltmeter. This instrument consists of a series of current-limiting resistors and a calibrated 6.25-centimeter spark gap. Standard 60-cycle breakdown curves are available for calibrating the sphere gap. Since the humidity has no effect on the breakdown of the gap, it is only necessary to correct for relative air density when using this curve.

The high potential test is easy to conduct. It does, however, have some limitations which are important for a test engineer to keep in mind. These limitations are regulation and capacity. The regulation of the test setup is important to take into consideration, because it causes the output test voltage to vary with loading. Where the regulation is poor, direct readings with a spark gap voltmeter are required. A serious error that can enter into switchgear checking is due to capacity loading of high potential testing circuits. This phenomenon causes the output voltage of a transformer to be increased over its effective turns ratio, since it, in effect, increases the turns ratio of the transformer. Figure 16 shows a vector diagram of a transformer with capacity loading. It should be noted that the excitation voltage (E_2) is actually lower than the terminal output voltage. This error can occur only when measuring high capacity circuits, such as large groups of switchgear assemblies, at one time. Resistance loading of a high potential circuit causes the effective ratio of the high voltage transformer to be less than the calibrated ratio. This effect is shown in Figure 17.

Impulse test simulates surge conditions

Switchgear equipment must have a high impulse level in order to assure strength against the lightning strokes and switching surges reaching the switchgear equipment. Switchgear is tested according to standards which require an impulse test voltage wave of a specified shape and duration. All switchgear above the 600-volt class must pass a 1½ by 40 impulse voltage test. The time required for the voltage to start out from zero and reach 95 kv, the maximum for 13.8-kv class switchgear, is 1½ microseconds. The 40 represents the time in microseconds for the voltage to reduce to ½ value point at 40 microseconds.

The impulse testing lab schematic diagram is shown in Figure 18. The impulse lab consists of three major parts: the high voltage mechanical rectifier, the wave-form forming and charging network, and the electronic control circuit. The wave-form forming network is triggered by a spark gap consisting of two spheres which have a built-in spark coil. The spark coil initiates the breakdown of the spark gap and in turn triggers the wave-forming network. This circuit consists of resistors and capacitors. Its principal job is to change the stored dc voltage into a 1½ by 40 impulse wave. This is accomplished by charging and discharging capacitors through resistors at a predetermined RC time rate. The impulse voltage is automatically applied directly to the specimen under test.

In parallel with the device under test is a noninductive potentiometer. The potentiometer enables a small amount of the impulse voltage to be fed directly to the vertical

plates of the oscilloscope. The oscilloscope is especially designed for high voltage work and has special sweep circuits, a high voltage oscilloscope tube which requires 20 kv for anode supply, and a special screen which enables photographs to be taken. The high voltage is required on the anode of this tube in order to assure proper brightness at the high writing speeds. The sweep circuits are designed to be nonlinear so as to fit more closely to the impulse nonlinear speed of travel. An external source of dc voltage is used to calibrate the vertical deflection of the oscilloscope beam. This enables the test engineer to calculate the impulse voltage very accurately by comparing the dc calibration deflection with the impulse deflection. In order to synchronize the sweep with the impulse wave, it is triggered with the same voltage pulse that triggers the wave-forming network. Pictures of impulse tests are usually taken with a high speed camera, and it is possible to determine failure point by studying these oscillograms. Figure 19 shows a 1½ by 40 impulse, which is a good test. Figure 20 shows two tests on a specimen with corona breakdown.

Corona is characterized by a dip in voltage and then a rebuilding up to the original voltage level. It is usually predominant at the peak of the impulse or just after the peak. Figure 21 is a typical breakdown from conductor to ground. Figure 22 is a test on a specimen which shows a partial breakdown to ground. This would result when parts of a winding of a transformer would short out or if parts of a series insulation would short out.

While standard 60-cycle high potential tests can only indicate freedom from insulation defects, corona tests actually prove the design quality of the switchgear high voltage components. Corona-free design is the best assurance that insulation on breakers, bushings, bus, and instrument transformers will withstand years of service.

MORE LIGHT ON EARLY STEAM TURBINE HISTORY

Dear Mr. Allen:

I have read with interest your article "Steam Turbine History Highlights," as it appears in the Allis-Chalmers "Electrical Review."

Some statement in reference to early De Laval developments may be of interest to you as it reflects the early turbine industry. I have had access to some historical write-ups originating in Sweden, which give the very early history of Dr. De Laval's activity. From these data I give you below some of the high points.

The first intimation that Dr. De Laval was thinking of a steam turbine dates back to 1876, where his personal notes cover a machine of that type. In 1886, he had the first thought of the impulse type of turbine, where he had come to the conclusion that an expanding nozzle was needed in order to get the full benefit of velocity from liberated energy in the steam.

In 1883, he built a reaction type of turbine operating at 42,000 rpm and found it was not a practical unit for commercial application. A number of small units were built and used for driving the cream separator.

Experiments with single-stage De Laval turbines also covered research on flexible shafts as well as double helical gears. These experiments were carried out in 1886 to 1890.

The finished design of the first single-stage De Laval turbine, including the use of the expanding nozzle, flexible shaft and double helical gears, was tested in 1890, and at that time designs had been completed with a series of different sized units, from 5 horsepower to 200 horsepower.

The first commercial contract, in competition with steam engines at that time, was in 1891, when two 5-horsepower turbogenerators were used for the illumination of an outdoor skating rink in Stockholm.

During his experiments in 1889, he had also produced and tested a great number of different types of turbine wheels, including two rows and three rows in combination. He also tested some wheels where the buckets were machined in the disc, very similar to the present Terry turbine.

The record shows that the first time the De Laval turbine was used for marine application was in 1892, when a 15-horsepower unit was built having two wheels — one for ahead operation and one for astern operation. Running tests were conducted in the summer of 1893. This unit operated at 16,429 rpm and had double helical gearing for a propeller speed of 330 rpm. It is interesting to note that this particular unit was built with the turbine case built for bottom exhaust to the condenser.

As far as our records go, the first steam turbine in the United States was a small single-stage De Laval turbine shipped to this country in 1891, and was used to convince the Patent Office that the expanding nozzle was an important detail in turbine design. This same unit was later exhibited at the World's Fair in 1893.

In 1897, a number of turbines were built in ratings of fifty horsepower and one hundred horsepower, each turbine being equipped with its own boiler where steam pressures as high as 3400 lbs were used. Some of these units were used in small power plants in connection with the Exposition in Stockholm in 1897, and furnished the electric power for a certain section of the Exposition.

I thought possibly the above information would be of interest to you from a historical standpoint.

Very truly yours,

(Signed by) C. R. Waller
Director for Engineering
DE LAVAL STEAM TURBINE CO.

Editor's note: Mr. Allen's articles appeared in the second, third, and fourth quarters, 1953 issues.

SIMULATING HIGH ALTITUDE flight conditions — the sub-atmospheric pressure and ultrasonic speeds encountered by jet aircraft — this 1,000,000-cfm axial compressor rotor will be installed in the Ram Jet Addition of the Arnold Engineering Development Center, Tullahoma, Tennessee. Each of two identical compressors, functioning as exhausters, will be driven by 24,500-hp synchronous motors and 6000-hp wound-rotor motors used for starting and supplementing the main drive motors.

A Design Philosophy for General Purpose Motors

by **V. B. HONSINGER**
Engineer-in-Charge
Apparatus Development Laboratory
Allis-Chalmers Mfg. Co.
Norwood Works

REDUCING PHYSICAL SIZE without changing performance is the goal of the current National Electrical Manufacturers Association rerate program for induction motors from 1 to 30 horsepower. Meeting these new specifications calls for an analytical understanding of NEMA standards as well as a knowledge of design procedures.

Stated by themselves, NEMA standards are specified numbers which express limiting conditions that inherently satisfy mechanical and electrical needs for particular requirements. To the designer, each electrical limit defines a system of points on a line; and when two of the requirements or limits are related, a two-dimensional system of points defining a surface or region is formed. This region represents the possible variations of design constants which are compatible with the NEMA standards. As each requirement is superimposed, it narrows the region — or may even show incompatibility with the previous requirements.

In any case, performance specifications of induction motors involve several key indices which shape the design. For Design B motors, NEMA standards define these five limiting conditions or values:

1. Minimum locked-rotor torque (T_s)
2. Maximum locked-rotor amperes (I_s)
3. Minimum breakdown (maximum torque) (T_m)
4. Maximum full-load slip ($s = .05$)
5. Maximum full-load temperature rise

Within the prescribed limits of these requirements there are an infinite number of possible motor designs, and those that excel in one or more features are sought out by designers.

Some induction motor performance requirements are interdependent. This is obvious from performance equations. Consider, first, the equation for motor leakage impedance, in terms of the symbols defined in Figure 1, if skin effect for the rotor cage is ignored. The leakage reactance components of the primary and secondary are grouped together and called x. The resistive components, r_1 for the primary and r_2 for the secondary, are distinguished from each other because the value of r_2 depends on several NEMA standards. The leakage impedance is:

$$z^2 = (r_1 + r_2)^2 + x^2 \qquad (1)$$

In this, z and r_2 are limited by NEMA standards, and thus the equation reduces to a function $f\ (r_1, x)$. The form of the equation is that of a circle having radius z with the center at point $P\ (-r_2, o)$.

Specifically, the limit of z is given by maximum permissible locked-rotor current if the effect of no-load current is neglected. This omission will not significantly affect the basic conclusions.

$$z \geqq \frac{V}{I_s} \text{ where } I_s \text{ is maximum}$$

The magnitude of r_2 falls between two limits. The first is determined by locked-rotor torque and ampere requirements, while the second is determined by motor slip.

$$r'_2 \geqq \frac{T_s n_s}{7.04\, m_1\, (I_s)^2} \quad \begin{matrix} T_s \text{ is minimum} \\ I_s \text{ is maximum} \end{matrix}$$

and

$$r''_2 \leqq \frac{T\, n_s\, s}{7.04\, m_1\, (I_2)^2} \quad s \text{ is maximum}$$

These inequalities together with the functional relationship $f\ (r_1, x)$ define a region in which the design must fall. In this case, because z is minimal, the region is the part *exterior* to the circle, as shown in Figure 2.

Expressing maximum torque graphically

The next step in determining the compatible design region is the graphic expression for maximum or breakdown torque:

$$T_m = \frac{7.04}{n_s} \quad \frac{m_1 V^2}{2\,(r_1 + \sqrt{r_1^2 + x^2})} \qquad (2)$$

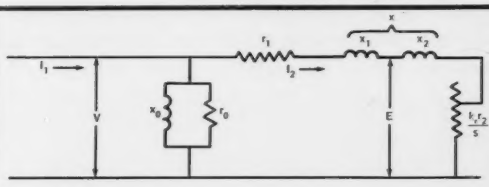

r_1 = primary resistance.
r_2 = secondary resistance at zero or small frequency.
k_r = factor to account for skin effect in rotor cage.
x_1 = primary leakage reactance.
x_2 = secondary leakage reactance.
$x = x_1 + x_2$
$z = (r_1 + r_2) + jx$
I_s = primary locked-rotor current $\approx V/z \ldots z_0 > > z$ and $s = 1 \ldots$ approx. $I_s \approx I_{2s}$.
I_{2s} = secondary locked-rotor current $= V/z$.
T_s = locked-rotor torque $= \frac{7.04\, m_1\, I_s^2\, (k_r r_2)}{n_s}$ (lb-ft).
T_m = maximum torque.
T = full-load torque.
m_1 = number of phases.
n_s = synchronous rpm.
I_1, I_2 = full-load primary and secondary current.
s = slip.
V = primary voltage per phase.
E = secondary voltage per phase.

SYMBOLS AND DEFINITIONS used in this article. **(FIG. 1)**

This equation likewise is a function $f(r_1, x)$ and transforms into a standard parabola

$$x^2 = -4\,\frac{\delta}{2}\left(r_1 - \frac{\delta}{2}\right) \qquad (3)$$

where

$$\delta \leqq \frac{7.04\, m_1 V^2}{2 n_s T_m} \quad \begin{matrix} T_m \text{ is minimum} \\ \therefore\ \delta \text{ is maximum} \end{matrix}$$

The value of δ is determined by the minimum limit for maximum torque. In other words, δ is maximal and the region so defined is *interior* to the parabola. Figure 3 shows this condition.

Combining the circle and parabola and restricting the design to positive values, a region bounded by the circle, parabola and x, r_1 axes is obtained. This is shown in Figure 4. All motors falling into this region will satisfy the first four of the five requirements previously listed.

Reducing the compatible region

We have derived elsewhere the somewhat qualitative formula:

$$\eta \cos\theta \approx \frac{(I_{2s}/I_1)^2}{(T_s/T)}\,(1-s)\,s k_r \qquad (4)$$

We are supposing at this stage that skin effect for the rotor cage is unity, $k_r = 1$ . . . later this will be reconsidered. It is requisite to design for high motor efficiencies as well as power factors. Satisfactory temperature rise, service factor, life, cost of operation — all are dependent particularly upon high efficiencies as well as, but to a lesser degree, upon high power factors. In order to obtain a high product $\eta \cos\theta$, it is clear that as a general criterion:

1. Percent locked-rotor torque must be minimum.
2. Percent locked-rotor current must be maximum.

This is exactly converse to the specified limits on locked rotor torque and amperes. Consequently, motors are designed to approach the limits as closely as is feasible within manufacturing and application tolerances. In this manner, motors can be designed that will excel in efficiency and power factor insofar as these are affected by locked-rotor torque and ampere requirements. In addition, the most that can be done to reduce temperature rise (the fifth requirement) will have been accomplished.

The new region is now very much limited. In fact, in the most technical sense, it has been reduced from a surface to a curve, which is shown in Figure 5 as a very narrow island just outside the z radius. Since it falls entirely within the larger region of compatibility, this curve is compatible with the first four requirements. Other problems have also been clarified and several more requirements of the standards automatically cared for. For example:

1. Maximum torque of the motor will be over the minimum limit.

2. Motor slip will not only be under the maximum limit but is now fixed by the formula:

$$r_2 = \frac{T_s n_s}{7.04\, m_1\, (I_s)^2}$$

Secondary locked-rotor current can be substituted for I_s in this formula.

Finally, only a specification of either r_1, x or the ratio r_1/x is needed to render the design unique. T. C. Lloyd has illustrated the dependency of the ratio r_1/x on lamination design of the stator and rotor. The design of these members, however, is a part of a different and more detailed viewpoint than this broad analysis.

These conclusions are valid only when equations (1) and (2) are valid. If, for example, a motor rotor is given an extremely high skew, the motor can take on radically different characteristics and not exhibit any distinct value for maximum torque or show a reversal of curvature in its speed-torque curve. Equation (2) would not be valid in this case.

Influence of skin effect

Skin effect in rotor bars increases rotor resistance and decreases rotor slot reactance as frequency is increased. At locked rotor, rotor frequency is line frequency and skin

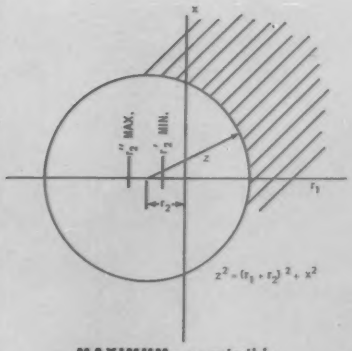

MAXIMUM permissible full-load slip restricts the center position of the locked-rotor limiting circle, while locked rotor amperes and torque define an exterior region. **(FIGURE 2)**

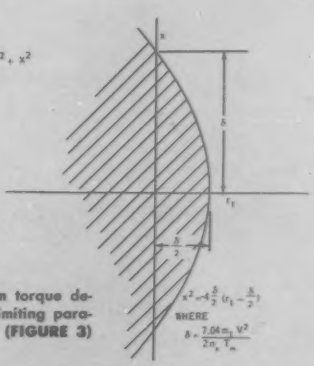

BREAKDOWN or maximum torque defines a region within this limiting parabola of maximum torque. **(FIGURE 3)**

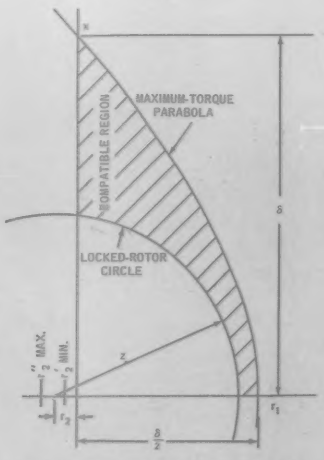

COMPATIBLE REGION satisfies four basic requirements: locked-rotor amperes and torque, maximum torque, and full-load slip. **(FIGURE 4)**

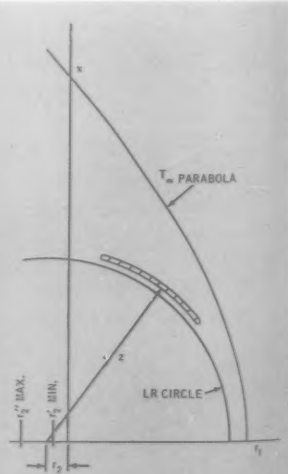

EFFICIENCY times power factor is maximum, full load slip is low and maximum torque sufficient within a narrow island as close to the locked-rotor circle as feasible. **(FIGURE 5)**

effect can be large for deep bar rotors, while at the slip of maximum torque the rotor frequency is small and so is skin effect. Since skin effect can alter a design quite radically, it must be given realistic consideration. To determine the extent skin effect will alter the compatible design region, the following formula can be used. In this equation, quantities x_s and z_s are leakage reactance and impedance with full skin effect, as at locked rotor, while x and z are these values at smaller frequencies (in this particular case, at the slip of maximum torque). Further, k_r modifies r_2 to include skin effect where r_2 is the rotor cage resistance at zero frequency. Thus at locked rotor with full skin effect equation (1) becomes:

$$z_s^2 = (r_1 + k_r r_2)^2 + x_s^2 \qquad (5)$$

while at maximum torque with partial skin effect equation (3), in the form below, has variables x and r_1 different than in equation (5)

$$x^2 = -4\,\frac{\delta}{2}\left(r_1 - \frac{\delta}{2}\right)$$

but the latter is transformed into a function $f\,(x_s, r_1)$ by simple algebraic manipulation

$$x_s^2 = -4\,\frac{\delta}{2}\left(r_1 - \frac{\delta}{2}\right)\left(\frac{x_s}{x}\right)^2 \qquad (6)$$

Equations (5) and (6) are now expressed by the same variables, and the factor $\frac{x_s}{x}$ in equation (6) becomes a reduction factor.

We also have for intercepts of the maximum torque parabola, equation (6):

when $x_s = 0 \ldots\ldots r_1 = \delta/2$

when $r_1 = 0 \ldots\ldots x_s = \pm\ \delta\left(\frac{x_s}{x}\right)$

Equation (5) does not alter the locked-rotor circle but simply redefines the position of its center as $k_r r_2$ where this value is a more generalized value of rotor cage resistance than previously given.

Parabolic equation (6) is altered in any case. The intercept on the x_s axis is now $\pm\,\delta(x_s/x)$ where $x_s/x < 1$, while the r_1 intercept remains as before $\delta/2$. Thus the effect is to narrow the compatible region, as shown in Figure 6; however, the reduction is not great. Skin effect on total leakage reactance is not large, since only rotor slot reactance, one of the half-dozen components included in x_s, is affected. On the other hand, skin effect for rotor resistance is large: k_r can be two or more and is the main source of design alteration.

The compatibility equation

It has been assumed up to this point that the circle and parabola *limiting* curves have no common points or intersections. There will be no intersections if the quantity

$$(\delta/2 + k_r r_2 - z_s) \geqq 0 \qquad (7)$$

Only essentially pure NEMA elements are involved in the components of this equation:

$$\delta/2 = \frac{7.04\, m_1 V^2}{4\, n_s T_m}$$

$$z_s = \frac{V}{I_s}$$

$$k_r r_2 = \frac{T_s n_s}{7.04\, m_1\, (I_s)^2}$$

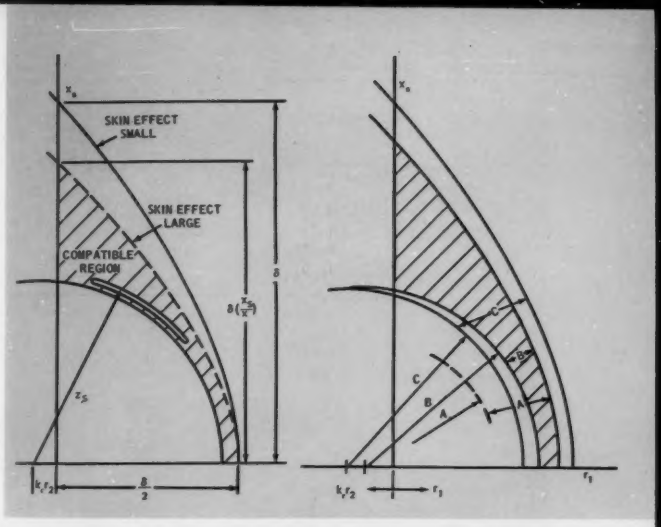

SKIN EFFECT narrows the compatible region without encroaching on the island of maximum η cos. θ. **(FIG. 6)**

RELATIVE compatible regions for Design A, B, and C 5-hp, 1750-rpm 440-volt, three-phase 60-cycle motors. **(FIGURE 7)**

If this quantity $(\delta/2 + k_r r_2 - z_s)$ is zero or any positive number, the requirements are compatible. The converse is not true. If the quantity is a negative number, compatibility may still exist. Since the quantity can be proven positive for all of the popular Design B motors designated in NEMA standards by inserting limits for T_s, I_s, and T_m (see Table I), it is called the "compatibility equation." The components also determine the limiting circles and parabolas.

Figure 7 shows 5-hp, 1800-rpm motors of A, B and C designs. Compatibility clearly exists for all three motors — all of which exhibit distinct breakdown or maximum torque. These considerations do not apply to Design D motors which have no breakdown torque specifications and do not necessarily exhibit a distinct reversal in curvature of the speed-torque curve.

Compatibility of slip with locked-rotor torque and amperes

NEMA standards define two separate rotor cage resistances (quite apart from the single value existing in the actual rotor itself) which have been designated as r''_2 and r'_2. The assumption up to this point has been that the value of rotor resistance r''_2, corresponding to maximum permissible slip, is greater than or equal to resistance r'_2, corresponding to permissible locked-rotor torque and amperes. This is not necessarily true. If an extremely large locked-rotor torque together with a very low slip were specified, a condition impossible to meet could result. Compatibility between these two resistances must exist quite aside from the other compatibility condition previously discussed. The two resistances r''_2 and r'_2 confine the center of the locked-rotor circle in Figures 2, 4 and 5. If $r''_2 < r'_2$ (the converse is shown in these Figures), then the motor slip limit cannot be satisfied when the locked-rotor torque and ampere limits are satisfied. Compatibility will exist when the specifications are arranged so that $r''_2 \geqq r'_2$. Consider two determinate equations for r''_2 and r'_2.

$$r''_2 = \frac{T n_s s}{7.04\, m_1\, (I_2)^2} \text{ at full load}$$

$$k_r r'_2 = \frac{T_s n_s}{7.04\, m_1\, (I_s)^2} \text{ at locked rotor}$$

We shall certainly have $r''_2 \geqq r'_2$ when

$$r''_2 \geqq r'_2\, k_r \ldots \text{ because } k_r \geqq 1$$

The same result in a slightly modified form is obtained by dividing the determinate equations above, one by the other:

$$\frac{r''_2}{k_r r'_2} = \frac{(I_s/I_2)^2}{T_s/T}\, s \geqq 1$$

Consequently, $r''_2 \geqq r'_2$ when

$$\left(\frac{I_s}{I_2}\right)^2 s - \frac{T_s}{T} \geqq 0 \qquad (8)$$

If equation (8) is zero or any positive number, then the value of $k_r r'_2$ is smaller than r''_2 and, of course, r'_2 by itself is still smaller. Equation (8) thus penalizes, possibly unnecessarily so, the probability of compatibility of these two types of resistance limits. Suppose, for example, equation (8) is not satisfied or is negative. Compatibility may still be caused to exist through use of the rotor *resistive* skin-effect factor k_r. Taking as the limit of compatibility $r''_2 = r'_2$, then instead of equation (8) we have, with but slight algebraic manipulation,

$$k_r = \frac{T_s/T}{(I_s/I_2)^2} \quad \frac{1}{s} \qquad (9)$$

This is the value of the rotor cage resistive skin-effect factor required to insure that both slip and locked-rotor torque and amperes can be obtained from one rotor dc resistance $r''_2 = r'_2$.

It is generally not necessary to resort to the extreme of this case, which could mean that the slip is at the limit of .05. However, the ramifications of equation (9) mean that the center of the locked-rotor circle may be designated as $k_r r_2$ as in Figure 6, with no loss in generality and with only little reduction of the "compatibility region." The locked-rotor circle radius, itself, is an independent specified value having to do with $k_r r_2$ only in the way the values $k_r r_2$, r_1 and x_s are prorated into z_s. True, the larger the *resistive* factor k_r, the smaller the *reactive* skin-effect factor. However, this effect is not vital, since the reactive factor, here designated as x_s/x, influences only one of a half-dozen of the constituent leakage reactance components, and therefore has only a relatively medium effect.

Equation (8) is satisfied for many NEMA Design B motors, and those which do not satisfy the equation are easily corrected by use of skin effect or deep bar rotors. This is sometimes desirable to improve efficiency; however, in extreme cases power factor, which is reduced somewhat by use of deep bar rotors, will be unduly impaired.

Manufacturing tolerances must be considered

From these considerations, generalized design objectives compatible with NEMA standards become apparent, particularly for the popular Design B motors. Locked-rotor torque and amperes, for example, should be as near these limits as manufacturing tolerances permit. A practice which has worked successfully is to design locked-rotor torque slightly over, and locked-rotor amperes slightly under the permissible limits. When this is done, breakdown torque will be over the minimum permissible value, and motor slip, except in very exceptional cases, will be less than 5 percent, which is the maximum permissible value for designs A, B and C. In addition, the product of efficiency and power factor, insofar as it is affected by locked-rotor torque and ampere specifications, will be maximum.

On the other hand, 220-volt motors that are to be rated for 208 volts as well must have a locked-rotor torque at least 12 percent over the NEMA standard for 220 volts if they are to meet NEMA standards at 208 volts. Such considerations as this enter into some cases.

Motors that greatly exceed locked-rotor torque for a given application will probably be low in efficiency and high in operating costs. In addition, original cost will probably be higher because more copper will be required.

Consequently, good design practice is to adhere as closely as possible to the locked-rotor torque and ampere limits of NEMA standards for motors and generators.

TABLE I — Design-B Motors . . . Specifications Derived from NEMA

2 — Pole Motors — 440 Volts $n_s = 3600$, $n_{f1} = 3500$

HP	T_s%	I_s	T_m%	δ/2	Z_s	$k_r r_2$	$\frac{\delta}{2} - Z_s / k_r r_2$
2	175	22.5	250	12.620	11.280	1.768	3.108
3	175	30.0	250	8.420	8.460	1.495	1.455
5	150	45.0	225	5.600	5.640	.945	.905
7½	150	60.0	215	3.910	4.230	.800	.480
10	150	75.0	200	3.160	3.390	6.82	.452
15	150	110.0	200	2.105	2.310	.476	.271
20	150	145.0	200	1.580	1.750	.365	.195
25	150	182.5	200	1.263	1.390	.288	.158
30	150	217.5	200	1.053	1.168	.244	.126
40	135	290.0	200	.788	.875	.164	.077

4 — Pole Motors — 440 Volts $n_s = 1800$, $n_{f1} = 1740$

HP	T_s%	I_s	T_m%	δ/2	Z_s	$k_r r_2$	$\frac{\delta}{2} - Z_s / k_r r_2$
1	275	12.0	300	20.900	21.150	4.911	4.661
1½	265	17.5	300	13.920	14.500	3.340	2.760
2	250	22.5	275	11.400	11.300	2.550	2.650
3	250	30.0	275	7.100	8.460	2.150	1.270
5	185	45.0	225	5.575	5.640	1.178	1.013
7½	175	60.0	215	3.890	4.230	.940	.600
10	175	75.0	200	3.135	3.385	.800	.550
15	165	110.0	200	2.090	2.311	.527	.306
20	150	145.0	200	1.568	1.750	.367	.185
25	150	182.5	200	1.253	1.390	.290	.153
30	150	217.5	200	1.045	1.168	.245	.122

6 — Pole Motors — 440 Volts $n_s = 1200$, $n_{f1} = 1150$

HP	T_s%	I_s	T_m%	δ/2	Z_s	$k_r r_2$	$\frac{\delta}{2} - Z_s / k_r r_2$
¾	175	9.0	275	30.200	28.200	4.200	6.200
1	175	12.0	275	22.650	21.150	3.150	4.650
1½	175	17.5	275	15.050	14.500	2.225	2.775
2	175	22.5	250	12.420	11.290	1.792	2.922
3	175	30.0	250	8.290	8.460	1.515	2.645
5	160	45.0	225	5.530	5.640	1.023	.923
7½	150	60.0	215	3.860	4.225	.811	.446
10	150	75.0	200	3.110	3.385	.690	.415
15	140	110.0	200	2.070	2.305	.451	.216
20	135	145.0	200	1.555	1.750	.334	.139
25	135	182.5	200	1.220	1.390	.268	.098

8 — Pole Motors — 440 Volts $n_s = 900$, $n_{f1} = 860$

HP	T_s%	I_s	T_m%	δ/2	Z_s	$k_r r_2$	$\frac{\delta}{2} - Z_s / k_r r_2$
½	150	6.0	250	49.600	42.300	5.415	12.715
¾	150	9.0	250	33.100	28.200	4.600	9.500
1	150	12.0	250	24.850	21.150	2.710	6.410
1½	150	17.5	250	16.570	14.500	1.913	3.983
2	150	22.5	225	13.730	11.300	1.540	3.970
3	150	30.0	225	9.200	8.460	1.300	2.040
5	130	45.0	225	5.940	5.640	.834	1.134
7½	125	60.0	215	3.850	4.230	.677	.297
10	125	75.0	200	3.100	3.385	.577	.292
15	125	110.0	200	2.070	2.305	.403	.168
20	125	145.0	200	1.550	1.750	.310	.110

new

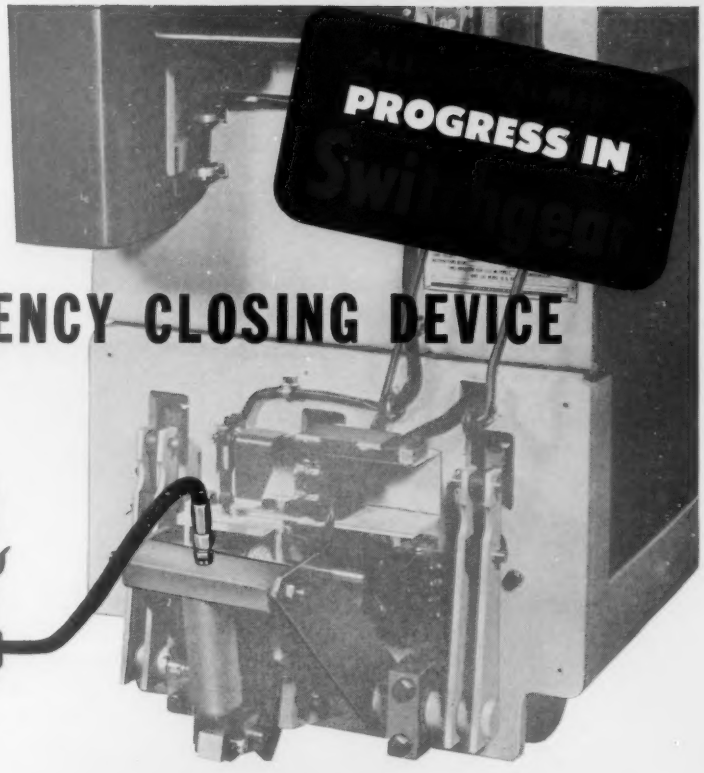

EMERGENCY CLOSING DEVICE

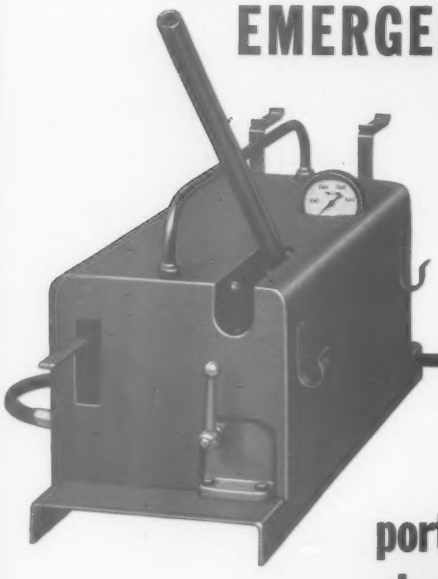

portable unit provides full-speed closing of air magnetic breakers

Here's a safe, reliable method of emergency closing an air magnetic breaker onto an energized line where no source of control power is available.

The *Pneu-Draulic* closing device weighs only 40 pounds and can be attached in less than 30 seconds. Its small size (8 x 14 x 10 inches) permits storing near breakers for instant availability. Only one device is needed for all Allis-Chalmers breakers of one type.

Basically, the *Pneu-Draulic* closing device is similar to that in the *Pneu-Draulic* operator for high capacity breakers. Only two moving parts are used to close breaker.

For more information, call your nearby A-C district office or write Allis-Chalmers, Milwaukee 1, Wis.

A-4268

WHY USE THIS CLOSER?

Because it is safe, reliable and fast. An air breaker closing on an energized line must be closed at normal speed. Using the usual manual emergency handle this cannot be done. This device affords the necessary speed.

WHEN DO YOU NEED THIS CLOSER?

Whenever any trouble occurs in the source of control power to the breaker. For example: failure of fuses, solenoid, rectifier, relays, wiring, control switch, or control power transformer.

Pneu-Draulic is an Allis-Chalmers trademark.

ALLIS-CHALMERS

T. H. Bloodworth
Hawley Works

How Long is 50 Years?

In the history of electric power, 50 years is a long time, for electricity was an infant in 1904 when Allis-Chalmers entered the steam and hydro-electric turbine manufacturing fields. But viewed as less than a single life span, 50 years seems a short time for the fabulous progress that has been made in the electric power field.

Only 50 years ago, A-C announced its readiness to build steam turbine units up to 10,000 kw "if required." Today, operation-proved *supercharged* generators and close-coupled cross-compound steam turbine designs have set a practical pattern for ratings up to 500,000 kw. In hydraulic turbines, production began with a 1250-hp, 88-ft hd unit; now top ratings are set by shipping considerations rather than design limitations.

Allis-Chalmers entry into the turbine field in 1904 was a natural step, because A-C had already established an enviable reputation in the manufacture of steam engines and other power equipment. Through the intervening years, Allis-Chalmers has continued to pioneer in the building of a wide, integrated range of power producing and utilization equipment.

A-4348

1904 **50** 1954
YEARS
Steam and Hydraulic
TURBINE
Manufacture

1862 *Mill-drive water wheels* 1869 *Steam engines*
1882 *Surface condensers* 1883 *Belted dynamo drives*
1892 *Direct-coupled engine-driven generator units*

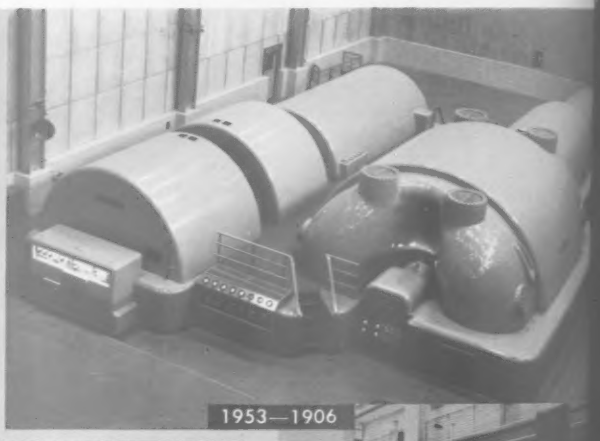

1953—1906

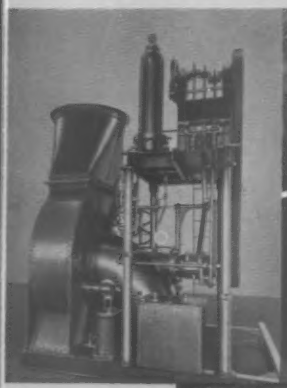

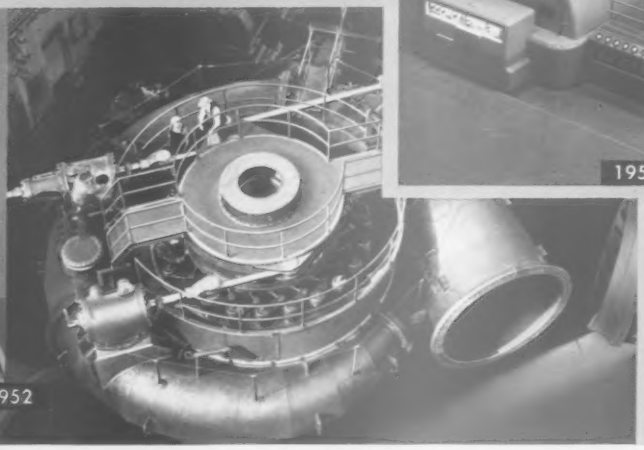

1904—1952

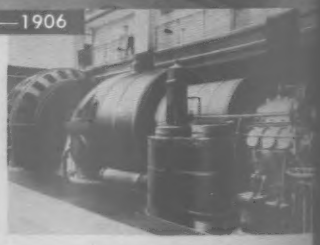

ALLIS-CHALMERS

A-C ALLIS-CHALMERS

SERVING INDUSTRY SINCE 1847